High-resolution satellite mapping of particulate pollution ($PM_{2.5}$) hotspots over Bhubaneswar and other non-attainment cities over Odisha

STATE POLLUTION CONTROL BOARD
ODISHA

SCHOOL OF EARTH, OCEAN AND CLIMATE SCIENCES
INDIAN INSTITUTE OF TECHNOLOGY BHUBANESWAR

January 2023

This page is intentionally left blank

Executive Summary

The rapid industrial and economic growth over the Indian subcontinent has led to increased air pollution specifically particulate matter. These tiny particles of size less than 2.5 µm ($PM_{2.5}$) are found to have adverse impact on public health and various other societally relevant issues such as anthropogenic climate change. The rapid population growth coupled with rural to urban migration is expected to change the urban share of the global population from 55% to 68% by 2050. India alone is expected to lead this transition with the addition of around 416 million, with countries like China and Nigeria trailing behind (United Nations, Department of Economic and Social Affairs, Population Division, 2019). This implies that Indian cities are vulnerable to increased air pollution and its impacts thereof. The National Clean Air Program (NCAP), initiated by the Ministry of Environment, Forests and Climate Change (MoEF&CC) of the Government of India (GoI), has identified more than a hundred cities as non-attainment in terms of their air quality. Seven of these cities are in the state of Odisha. The primary objective of this program is to reduce particulate matter pollution levels by up to 30% in a couple of years. The policy decisions to initiate these reductions require a critical understanding of the spatio-temporal distribution of particulate matter air pollution and their sources in each of these non-attainment cities (NAC). As a part of this initiative, with support from the State Pollution Control Board (SPCB), Odisha, the Indian Institute of Technology Bhubaneswar (IIT-BBS) undertook a project to develop high-resolution $PM_{2.5}$ maps (hotspot identification) using satellite data over seven non-attainment cities in Odisha. This report summarises the outcome of the project.

This page is intentionally left blank

Acknowledgements

The authors acknowledge the State Pollution Control Board, Odisha, for providing the necessary funding support and ground-based observational data to carry out this project. The support and encouragement from Dr K Murugesan IFS (Member Secretary) and Dr Nihar Ranjan Sahoo (Chief Environmental Engineer) are gratefully acknowledged. The PI thanks Dr Simanchala Dash and Ms Subhadarshini Das for their enthusiastic support during this project. We thank the Ministry of Environment Forests and Climate Change (MoEF&CC) for initiating the National Clean Air Program (NCAP) through the Central Pollution Control Board (CPCB) and State Pollution Control Board (SPCB). SPCB Odisha, through NCAP, sponsored this project. Dr Tanmoy Mukherjee, Mr Soumya Satyakanta Sethi and Mr Ruthvik Galem are acknowledged for their scientific contribution.

This page is intentionally left blank

List of Figures

Table of Contents

This page is intentionally left blank

Annual and Seasonal Maps of $PM_{2.5}$ over Seven Non-Attainment Cities of Odisha

1. Introduction

The mandate of the National Clean Air Programme (NCAP) under the stewardship of the Ministry of Environment, Forests and Climate Change of the Government of India envisage reducing air pollution by up to 20-30% of $PM_{2.5}$ and PM_{10} concentrations by 2024. The most important aspect to understand to achieve this goal is to know the sources of air pollution at the city and regional scales with sufficient spatio-temporal resolution. However, current ground-based measurement methodologies cannot provide such information even with high spatial coverage. The Indian Institute of Technology Bhubaneswar, with the support of the State Pollution Control Board (SPCB), Odisha, has undertaken a project to generate high-resolution Particulate Matter (PM) maps and identify the pollution hotspots over the seven non-attainment cities of Odisha. The mapping uses high-resolution satellite datasets (1x1 km spatial resolution) with daily temporal coverage over the study region. The project was initiated on 1st April 2020 to support NCAP objectives. This assessment report represents the outcomes of the project. Following the research reviews and goals, the report presents detailed discussions about the hotspots identified over the non-attainment cities.

2. Research Literature Review

2.1 Particulate Matters

The fine particulate matter with aerodynamic diameters less than 2.5 µm ($PM_{2.5}$) is one of the most harmful pollutants, which negatively affects human health and can cause premature deaths (Pope III et al., 2002; Brauer et al., 2012){“id”:”ITEM-2”,”itemData”:{“DOI”:”10.1001/jama.287.9.1132”,”ISSN”:”0098-7484”,”abstract”:”Context Associations have been found between day-to-day particulate air pollution and increased risk of various adverse health outcomes, including cardiopulmonary mortality. However, studies of health effects of long-term particulate air pollution have been less conclusive. Objective To assess the relationship between long-term exposure to fine particulate air pollution and all-cause, lung cancer, and cardiopulmonary mortality. Design, Setting, and Participants Vital status and cause of death data were collected by the American Cancer Society as part of the Cancer Prevention II study, an ongoing prospective mortality study, which enrolled approximately 1.2 million adults in 1982. Participants completed a questionnaire detailing individual risk factor data (age, sex, race, weight, height, smoking history, education, marital status, diet, alcohol consumption, and occupational exposures. $PM_{2.5}$ particles enter the alveoli, subsequently retained in the lung parenchyma (Dockery, 2014). Thus, it can create several cardiovascular and respiratory diseases and even lung cancer (Brook et al., 2010; Hoek et al., 2013). The global burden of disease study (GBD 2010) reported that $PM_{2.5}$ is the sixth most significant cause of premature death in the South Asian region (Lim et al., 2012). As per WHO, 13 out of 20 most polluted cities are in India (World Health Organization, 2016)one out of every nine deaths was the result of air pollution-rela- ted conditions. Of those deaths, around 3 mil- lion are attributable solely to ambient (outdoor. A recent study using the Modern-Era Retrospective Analysis for Research and Applications Version 2 (MERRA-2) model has shown that the $PM_{2.5}$ concentrations are always higher over the Indo-Gangetic plain throughout the year exceeding the air quality standards with the highest during the post-monsoon season (Navinya et al., 2020).

2.2 Atmospheric Aerosols

Atmospheric aerosols are small solid or liquid particles suspended in the atmosphere originating from both natural and anthropogenic activities. They can alter the energy balance of Earth and hence its climate. Aerosols can influence the climatic variability directly by scattering or absorbing solar radiation (Atwater, 1970; Ensor et al., 1971) and indirectly by affecting droplet concentrations and, therefore, cloud formations (Menon et al., 2002; Lohmann and Feichter, 2004; Takemura et al., 2005; Gu et al., 2012; Dipu et al., 2013; Ning et al., 2015). Several researchers have investigated the characteristics and behaviour of aerosol over the Indian region (Dey et al., 2005; Beegum et al., 2009; Vinoj et al., 2010, 2014)Trivandrum (8.55??N, 76.9??E, 3 m msl. It is reported that the increase of Aerosol Optical Depth (AOD) over the Indian region is ~2.5% per year (Krishna Moorthy et al., 2013), mainly as a consequence of increased anthropogenic activities.

The concentration of $PM_{2.5}$ is primarily measured at the surface level using ground-based instruments. However, along with point-based observation, aerosol loading can also be estimated on a large spatial scale using satellites. The aerosol column loading is typically measured as Aerosol Optical Depth (AOD), defined as the integrated extinction coefficient of aerosols over a vertical column of a unit cross-section. Therefore, satellite-derived AOD (which is also modified by ground-level $PM_{2.5}$) can be used to map the particulate concentration spatially over a particular region after ensuring the removal of other effects that may modulate AOD.

2.3 Mapping of $PM_{2.5}$ using Aerosol Optical Depth

Several researchers have attempted to map $PM_{2.5}$ using satellite-derived AOD across the globe (Wang and Christopher, 2003; Liu et al., 2004). Wang and Christopher (2003) initiated the PM mapping by utilizing the Moderate Resolution Imaging Spectrometer (MODIS) data using the linear correlation method. Chemical transport models (Liu et al., 2004) and day-specific mixed effect models (Lee et al., 2011)"ISSN":"16807316","abstract":"Epidemiological studies investigating the human health effects of PM 2.5 are susceptible to exposure measurement errors, a form of bias in exposure estimates, since they rely on data from a limited number of PM 2.5 monitors within their study area. Satellite data can be used to expand spatial coverage, potentially enhancing our ability to estimate location- or subject-specific exposures to PM2.5, but some have reported poor predictive power. A new methodology was developed to calibrate aerosol optical depth (AOD were introduced to estimate the PM concentrations. Several satellites, including the Multi-Angle Imaging Spectrometer (MISR) (Liu et al., 2007; Lee et al., 2011)"ISSN":"16807316","abstract":"Epidemiological studies investigating the human health effects of PM 2.5 are susceptible to exposure measurement errors, a form of bias in exposure estimates, since they rely on data from a limited number of PM 2.5 monitors within their study area. Satellite data can be used to expand spatial coverage, potentially enhancing our ability to estimate location- or subject-specific exposures to PM2.5, but some have reported poor predictive power. A new methodology was developed to calibrate aerosol optical depth (AOD, the Geostationary Operational Environment Satellite (GEOS) (Paciorek et al., 2008), the Sea-viewing Wide Field-of-view Sensor (SeaWiFS) (Van Donkelaar et al., 2015), the Ozone Monitoring Instrument (OMI) (Li et al., 2015) and the Cloud-Aerosol Lidar with Orthogonal Polarization (CALIOP) (Li et al., 2015) were earlier used for the PM mapping.

It is reported that meteorological parameters such as humidity and the height of the boundary layer are significant enough to affect and even invert the relationships between AOD and $PM_{2.5}$ (Zhang et al., 2018)there are numerous PM 2.5 sampling and monitoring facilities that rely on data from only representative points, and which cannot measure the data for the whole region of research interest. This provides the motivation for researching the methods of estimation of particulate matter in areas having fewer monitors at a special scale, an approach now attracting considerable academic interest. The aim of this study is to (1. The recent swift socio-economic growth over the south Asian region has led to increased anthropogenic aerosol emissions (like black carbon and sulphate). Countries like China and India are experiencing heavy pollution episodes in major urban areas. Several attempts have been made to infer the $PM_{2.5}$ concentrations from the AOD data over these regions. A recent study over China reported that the correlation between AOD and $PM_{2.5}$ is higher in the dry North. In contrast, it is lower over the humid southern region as the extinction efficiency of the hygroscopic aerosols has increased with higher humidity (Xin et al., 2017). A study has reported that $PM_{2.5}$ is highly correlated during wintertime over Delhi (Tiwari et al., 2015)IMD: a less traffic site and IITM: an urban background site. A nonlinear multi regression model study over Jaipur found a high correlation between estimated and observed $PM_{2.5}$ (Soni et al., 2018). Recent studies have also generated district-level $PM_{2.5}$ mass concentrations from AOD to evaluate the premature mortality rate due to $PM_{2.5}$ (Chowdhury and Dey, 2016; Chowdhury et al., 2018). Though several studies look at particulate matter distribution, seasonality, and its relationship with aerosol loading, not many studies have addressed the issue of city-scale hotspot identification using satellite datasets systematically.

3. Objective of the study

There are seven non-attainment cities in Odisha state – Angul, Balasore, Bhubaneswar, Cuttack, Kalinga Nagar, Rourkela, and Talcher. Though a few point-based monitoring stations are located around the city, it is crucial to identify the pollution hotspots on a spatial scale for better air quality management. PM_{10} and $PM_{2.5}$ are the primary pollutants of concern in all these cities. In addition, Odisha state lies in the path of Indo-Gangetic Plains (IGP) outflow with the possibility of it being affected by aerosols of long-range/remote origin. Therefore, it is essential to map and understand $PM_{2.5}$ over these rapidly urbanizing towns/cities, which may eventually pave the way for air pollution action plans to reduce local emissions and hence particulate matter concentrations at city scales.

The primary objective of this project is,

i. To generate $PM_{2.5}$ spatial maps from satellite-derived aerosol optical depth over Bhubaneswar city in the first phase and then expand to other non-attainment cities over Odisha.

ii. To understand the advantages and disadvantages of the existing methods of $PM_{2.5}$ mapping.

iii. Develop expertise and capability to generate $PM_{2.5}$ maps based on multiple satellite datasets that enable OSPCB to make quick policy decisions.

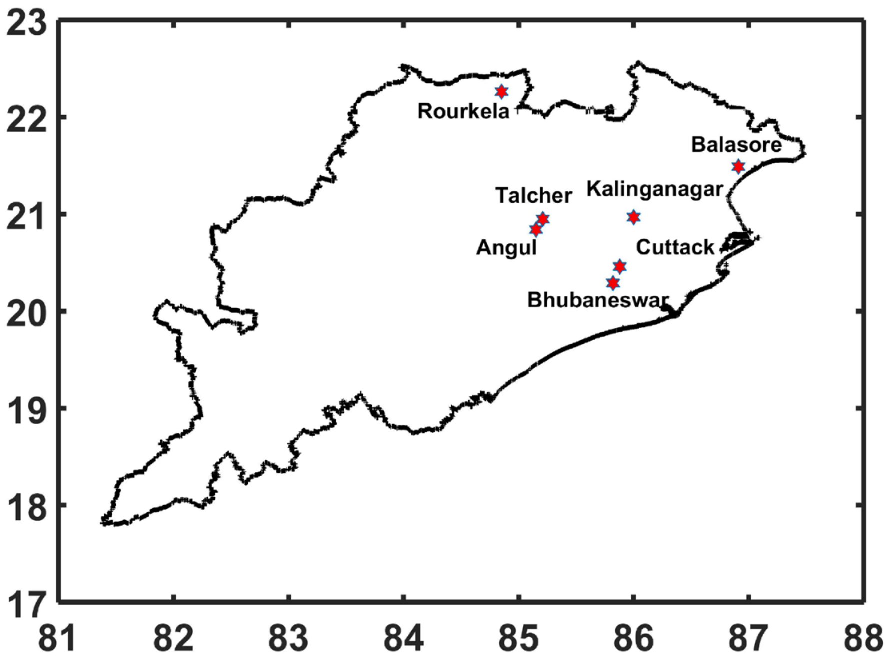

Fig. 1 Location of the non-attainment cities spread across the state of Odisha

4. Problems Associated with the satellite-based $PM_{2.5}$ mapping

Studies have reported that meteorological parameters such as relative humidity and height of the boundary layer are significant enough to affect and even invert the relationships between AOD and $PM_{2.5}$. (Zhang et al., 2018)there are numerous PM 2.5 sampling and monitoring facilities that rely on data from only representative points, and which cannot measure the data for the whole region of research interest. This provides the motivation for researching the methods of estimation of particulate matter in areas having fewer monitors at a special scale, an approach now attracting considerable academic interest. The aim of this study is to (1. A study found that aerosol type and height of the boundary layer are significant factors in predicting $PM_{2.5}$ levels over Nanjing (Han et al., 2015). Besides that, the satellites retrieved AOD has their own bias due to retrieval over different locations. Therefore, it appears that the relationship between Particulate Matter (PM) and AOD depends on site, particulate size distribution, composition, and vertical profile of aerosols. Several other factors (e.g. rainfall and winds) may also modulate and modify $PM_{2.5}$ mapping using column AOD. The climatic system of Bhubaneswar is characterized by high temperature and relative humidity. Due to its location, the city is influenced by mineral dust transport from the western deserts and sea-salt aerosols due to marine air intrusion due to its proximity (~ 60 km) to the Bay of Bengal (Mukherjee and Vinoj, 2020). All these factors may modify the AOD-PM relationship substantially.

In addition, the satellite datasets show an overall low bias compared to the observed AOD data over Bhubaneswar (Fig. 2a). Also, the climatological seasonality of the AOD from different satellites shows a different pattern (Fig. 2b). Therefore, only a systematic and critical investigation using different techniques and correction factors customized for particular regions may represent the $PM_{2.5}$ scenarios over Bhubaneswar city and/or Odisha state.

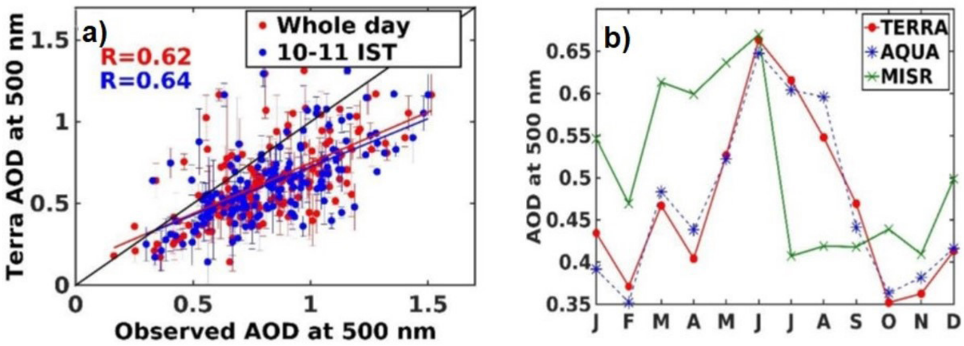

Fig. 2 Satellite data validation over Bhubaneswar (Source: Mukherjee and Vinoj, 2019)

5. $PM_{2.5}$ Mapping Methods

Mapping particulate matter at very high resolutions of 1x1 km spatial scale is attempted using two methods. One of the methods utilized the coarse resolution $PM_{2.5}$ mass concentrations simulated by the NASA chemical reanalysis system along with the high-resolution aerosols from satellites to develop grid-level or city-level relationships for $PM_{2.5}$ mass concentration. The other method uses statistical tools to create high-resolution maps using ground-based observation and satellite-derived data of various aerosol and meteorological parameters.

These methods have their inherent limitations. However, methods utilizing actual measurements are expected to reduce uncertainties/errors in these estimates. The present report used two different methods to produce the annual and seasonal maps of $PM_{2.5}$ mass concentrations over Bhubaneswar and other non-attainment cities using satellite-derived aerosol optical depth

(AOD) data. The methods are called the MERRA-MODIS (called the **Model-Satellite method**) and other statistical methods and are described in the following sections.

5.1 Model-Satellite Method (MERRA-MODIS Method)

The Modern-Era Retrospective analysis for Research and Applications Aerosol Reanalysis (MERRAero), provides the long-term dataset of 15 different tracers, including Black Carbons (BC), sulfate, dust, and sea salt. These datasets are estimated by carefully assimilating gridded aerosol optical measurements and global emission inventory into the climate modeling system. The current study utilizes the long-term data (2003-2018) of the various aerosol types to calculate the $PM_{2.5}$ over Bhubaneswar using the nearest model grid. The monthly MERRAAero reanalysis data of different aerosol species are used for the current analysis. These are first-cut particulate matter estimates to develop a city-specific mapping of $PM_{2.5}$ hotspots. Eighteen years (2001-2018) of MERRA data has been utilized to calculate the $PM_{2.5}$. The general form of the equation to arrive at the total PM mass for any size is given as follows:

Total PM = Inorganic ions + Organic matter + Black carbon+ Dust + Sea salt.

Following Hind et al., 2011, we determine the $PM_{2.5}$ mass using the equation given below,

$$[PM_{2.5}] = 1.375 \times [SO_4] + 1.8 \times [OC] + [BC] + [DU_{2.5}] + [SS_{2.5}] \quad (1)$$

Where, SO_4 = Sulphate.

OC = Organic Carbon.

BC = Black Carbon

$DU_{2.5}$ = Dust particles less than 2.5 microns.

$SS_{2.5}$ = Sea Salt particles less than 2.5 microns.

The MODerate Resolution Imaging Spectroradiometer (MODIS) provides Aerosol Optical Depth (AOD) data at 1 x 1-degree resolution. The calculated $PM_{2.5}$ is compared with the satellite AOD values to obtain an empirical relationship between AOD and $PM_{2.5}$. Figure 3 shows the correlation between MERRA-2 $PM_{2.5}$ and MODIS AOD in monthly and seasonal scales. Both monthly and seasonal data show significant correlations, indicating that the empirical equations generated based on model-derived data can be used to map the $PM_{2.5}$ over the study areas. It may be noted that daily datasets were not used in the present analysis to avoid large variability that may induce errors in the estimated slopes.

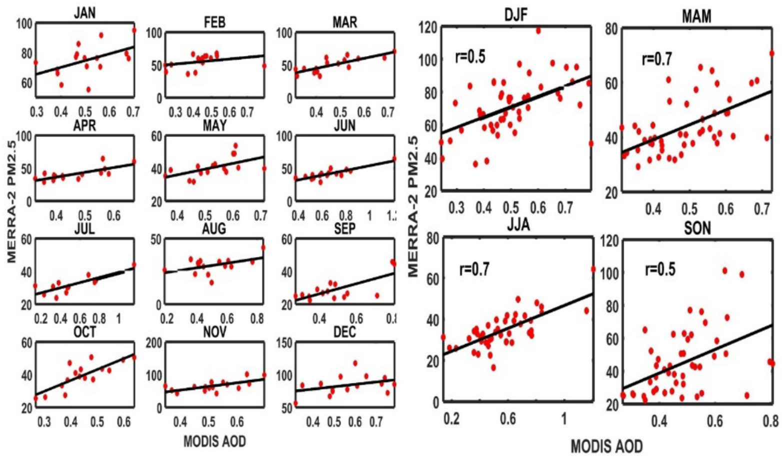

Fig. 3 Relationship between MERRA-2 derived model $PM_{2.5}$ and MODIS satellite AOD

With the equations derived, monthly, seasonal and annual maps of $PM_{2.5}$ were generated using MODIS level-2 1km AOD data (MCD19A2 version 6, from 2011-2019). The long-term AOD data were used to create annual, seasonal, and monthly average $PM_{2.5}$ maps. Figure 4 represents the schematic diagram of the model-satellite method (hereafter called the M-S method). Surprisingly, the JJA period has the best correlation pattern of all seasons. This indirectly indicates the possibility of long-range transport of particulate matter that may be influencing the AOD measurements even at ground level. During this period, the large-scale regional rainfall effectively removes these transported aerosols, constraining the local concentration of particulate matter to be more effective in creating optical attenuation and hence AOD. The other periods show typical patterns observed in such studies elsewhere.

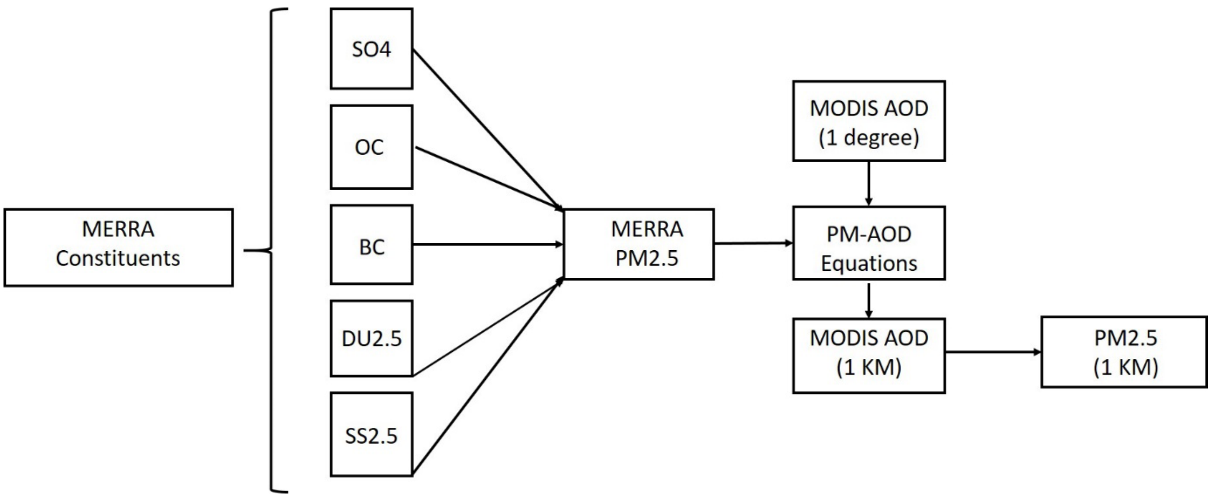

Fig. 4 Schematic showing the detailed workflow of the MERRA-MODIS Method (M-S Method)

5.2 Ground-Satellite Method (Ground-MODIS-Meteorology Method)

The method utilizes ground-based observation data of $PM_{2.5}$ provided by the State Pollution Control Board, Odisha (OSPCB). The empirical equations based on observed $PM_{2.5}$ and AOD were initially calculated (similar to the M-S method). However, the estimated $PM_{2.5}$ based on that equation shows a very insignificant correlation with the observed data (Fig.6a).

Several studies have reported that the AOD-PM relationship can be affected by numerous meteorological factors like relative humidity (RH) or the planetary boundary layer height (PBLH). Therefore, several parameters have been added sequentially, and the correlation improved eventually (Fig 6 b-d). Finally, a multiple linear regression equation with interaction terms has been calculated to obtain a significant relationship between AOD and PM over the study location.

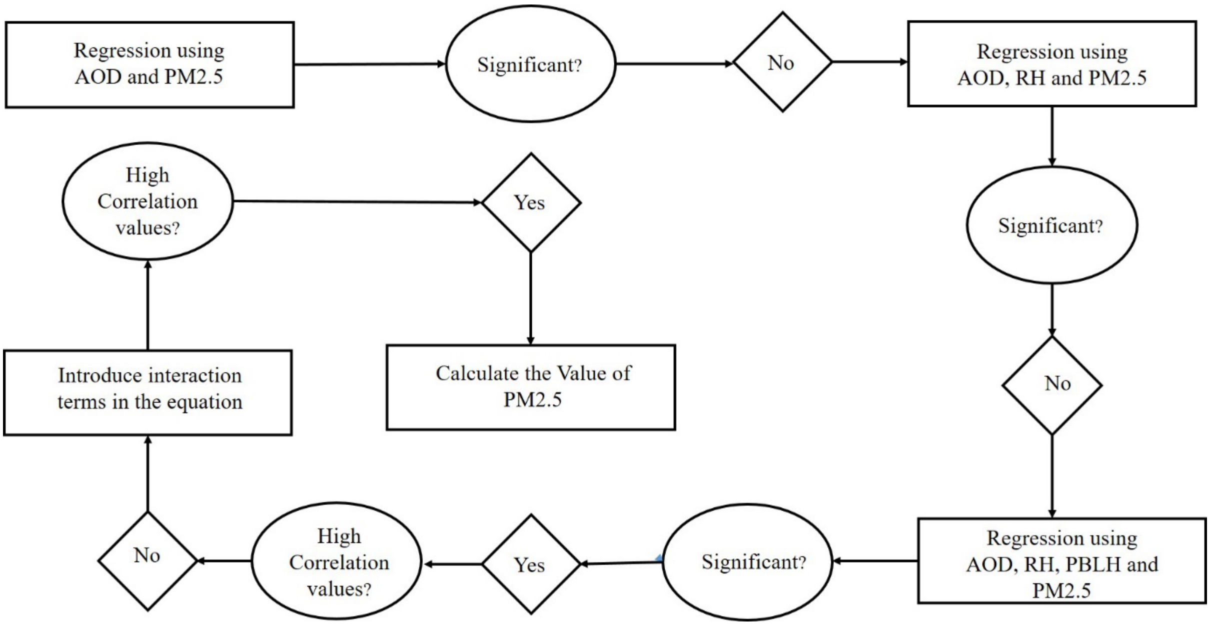

Fig. 5 Schematic showing the detailed workflow of the Ground-Satellite Method (G-S Method)

The AOD data is obtained from MODIS, while the $PM_{2.5}$ data is obtained from OSPCB. The RH and PBLH data is obtained from the National Centre for Medium-Range Weather Forecasting (NCMRWF) reanalysis datasets. The following multiple linear regression model is thus established,

$$\mathbf{PM_{2.5} = a_0 + a_1{*}AOD + a_2{*}RH + a_3{*}\ PBLH + a_4{*}\ AOD{*}\ RH + a_5{*}AOD{*}PBLH} \quad \text{(2)}$$

Where, a_0 to a_5 are respective coefficients.

The annual and seasonal equations are then generated separately. The yearly (annual) and seasonal maps are then created using the 1 km^2 high-resolution data. The comparison of estimated $PM_{2.5}$ with the ground-based measured $PM_{2.5}$ mass concentrations clearly shows the improvement in the estimates when meteorological parameters such as RH, PBLH, and their interactive terms are included. This indicates that simple calculations using ground-based $PM_{2.5}$ and AOD may not be sufficient to create spatial and temporal estimates of $PM_{2.5}$ mass concentrations at large spatial scales.

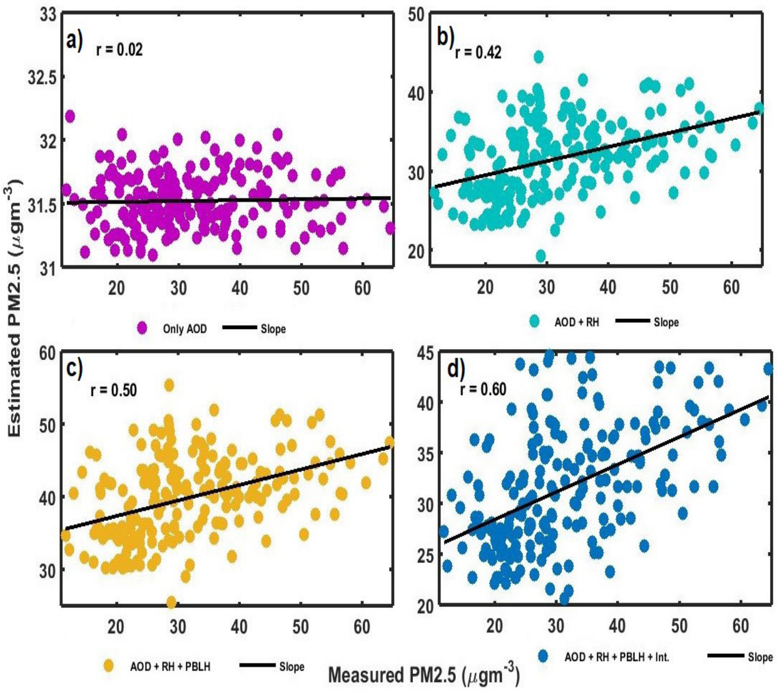

Fig. 6 Interrelation between observed and Measured $PM_{2.5}$ using a) raw $PM_{2.5}$ and AOD b) raw $PM_{2.5}$, AOD along with relative humidity (RH) c) $PM_{2.5}$ along with AOD, RH and PBLH d) $PM_{2.5}$ along with AOD, RH, PBLH and additionally interactive coefficient with RH, PBLH and AOD.

6. Description of the Non-Attainment Cities

6.1 Angul

Angul came into existence as a separate district on 1st April 1993. The district community has a population of around 1.2 million (census 2011). The area of the Angul district is 6232 km^2. The administrative headquarters of Angul is located in Angul city (20.84°N, 85.15°E). The town is well known as the Industrial capital of Odisha. The Angul city witnessed tremendous industrial growth in the past few decades as industries like National Aluminium Company Limited (NALCO) and Jindal Steel Power Limited (JSPL) set up their operations. Due to the large concentration of industrial units, Angul city is expected to show significant Spatio-temporal variability in particulate matter.

6.2 Balasore

Balasore is one of the coastal districts of Odisha located in the northern part of the State. With a total population of nearly 2.3 million (census 2011), Balasore city (21.49°N, 86.94°E) is the administrative headquarters of the Balasore district. The area of Balasore district is 3806 km^2.

The district is recognized for both industries and agriculture, such as paddy cultivation. The hot, humid climate and the presence of alluvial soil create favourable conditions for agriculture in this district. It is also one of the economically strong districts of Odisha state. Due to the high population and solid economic activities, Balasore is expected to show the signature of significant anthropogenic emissions.

6.3 Bhubaneswar

Bhubaneswar (20.29°N, 85.82°E) is one of the fastest-growing tier-2 cities in Eastern India with a nearly 0.85 million population (as per census 2011). The area of the city is around 422 km^2. The city has seen increased industrial activities since the 1990s due to changes in Government policies. It has emerged as an important trading and commercial hub with four major industrial areas around the city. Many small and medium industries and commercial residential developments account for a gradual increase of particulate matter over this region. Based on the ground measurement, a recent study reported high aerosol loading (annual average AOD is 0.7 ± 0.3) over this region (Mukherjee and Vinoj, 2020).

6.4 Cuttack

The former capital of Odisha state, Cuttack (20.46°N, 85.88°E), is the second-largest city with a population of ~ 0.6 million (as per census 2011). It is one of the oldest cities in the State and is famous for its silver filigree works. The area of the city is 192.5 km^2. It is known as the commercial capital of Odisha as it hosts several trading and business houses in and around the city. About 11 large-scale industries are situated in and around Cuttack, mostly in Choudwar and Athagarh. These industries include steel, power, automobile, alloys, fireclay, etc. Besides that, it is one of the leading textile hubs in eastern India. The heavy population and the large industrial areas clustered in a small area impact the city's air quality.

6.5 Kalinganagar

Kalinganagar (20.97°N, 86.00°E) is a planned industrial and modern town in the Jajpur district of coastal Odisha, India. The population of the area is nearly 50 thousand (www.indiagrowing.com). The projected area of Kalinganagar is around 177 km^2. The site is rich in iron ore. Many steel plants, including Jindal Steel and Tata Steel, are in various stages of implementation in this area. In partnership with the Government of Odisha, Tata Steel is committed to setting up a six million-tonne per annum integrated steel plant at Kalinganagar. Several other industries like Neelachal Ispat Nigam Limited, Jindal Steel, VISA Steel, etc., are located in this area.

6.6 Rourkela

With over 0.55 million population, the steel city of Odisha, Rourkela (22.22°N, 84.86°E), is the third-largest city in the state. The area of the city is around 102 km^2. Rourkela has a tropical climate and receives high rainfall during the Southwest monsoon (June – September) and retreating Northeast monsoon (December – January). One of the largest steel plants under the Steel Authority India Limited (SAIL) is located in the town. The plant produces more than 1.8 million tons of integrated steel. In addition, the city is also considered a reputed knowledge hub. Large steel plants and allied industries enhance the city's pollution level.

6.7 Talcher

Talcher (20.95°N, 85.21°E) is one of the four subdivisions of the Angul district of the Odisha state. As per the 2011 census, the area's population was around 41 thousand. A large thermal power plant by National Thermal Power Corporation is located in the city. The site is rich in minerals. The coal mines of Mahanadi Coal Field Limited are operating in the city.

7. Results and Discussions (M-S Method)

This section presents the annual and seasonal $PM_{2.5}$ maps of seven non-attainment cities generated using the M-S method. The $PM_{2.5}$ hotspots were also identified over these locations. These maps will be used only to identify hotspots and not to intercompare the $PM_{2.5}$ mass concentration estimates between the cities (see methods). Hence, the $PM_{2.5}$ estimates are only a relative measure for comparison and are not to be used on absolute terms. The spatial and temporal patterns are of excellent quality as AOD estimates from satellites are quality controlled. Only those quality assured datasets flagged as good are used in this analysis. The hotspots are identified as areas having $PM_{2.5}$ mass concentrations higher than the 70^{th} percentile of the spatial loading.

7.1 Annual and Seasonal $PM_{2.5}$ maps and Hotspots over Angul

The annual average of $PM_{2.5}$ over Angul shows high pollutant loading over the city **(~55 µgm^{-3})**. The area adjacent to Durga Vihar and Railway colony experiences $PM_{2.5}$ loading of more than ***60 µgm^{-3}***. Though the $PM_{2.5}$ does not show a wide range in the annual average, a few areas like ***Durga Vihar, Railway Colony, Budhi Thakurani, and Hata square*** can be identified as hotspots.

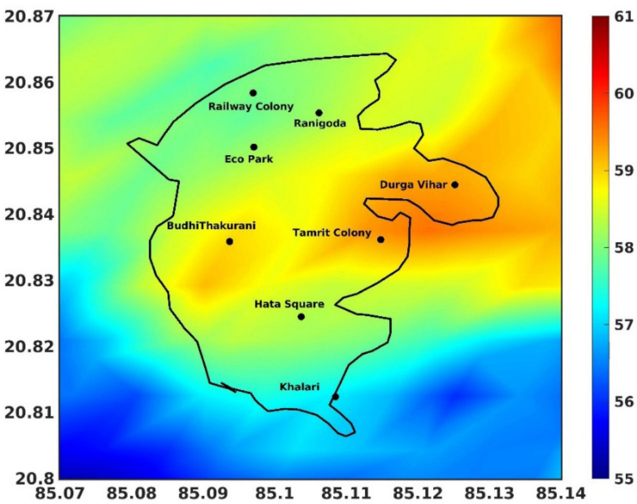

Fig. 7 Annual average concentration of $PM_{2.5}$ over Angul

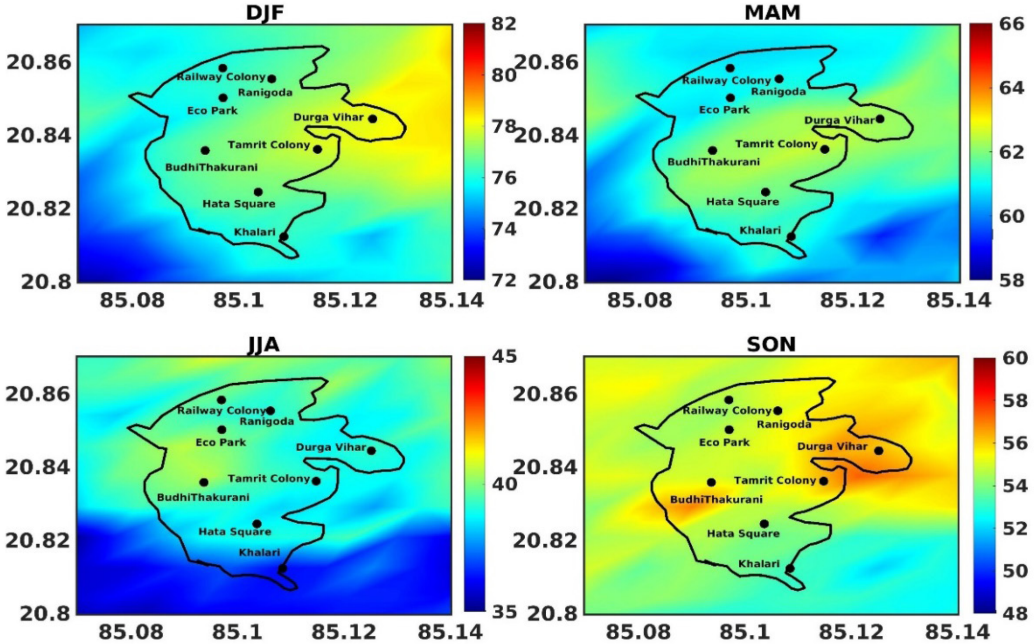

Fig. 8 Seasonal Concentration of $PM_{2.5}$ over Angul

The **figure 8** depicts the average seasonal concentration of $PM_{2.5}$ over Angul. It is noted that seasonally the concentration levels vary widely. However, the Eastern part of the city (adjacent to Durga Vihar, Tamrit Colony) shows higher values in all seasons. The highest values can be observed during winter, followed by pre and post-monsoon. It is important to note that even during monsoon, ***the values exceed 40 μgm^{-3}*** in a few places indicating the high pollution over the study region.

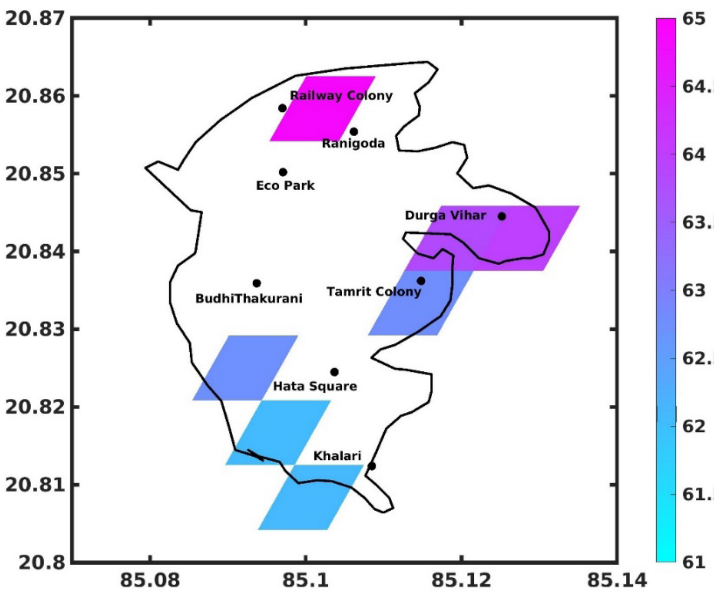

Fig. 9 Annual $PM_{2.5}$ hotspots over Angul

The 70 percentile value over Angul is ***61 µgm⁻³***. A significant intraseasonal variation in the number of hotspots can be observed. However, most of the hotspots can be identified during winter and post-monsoon periods. The hotspots can be listed as,

i. Area surrounding Railway Colony and Ranigoda.

ii. Tamrit Colony and adjoining industrial estate.

iii. Area surrounding Hari-Mohari Chhaka.

7.2 Annual and Seasonal $PM_{2.5}$ maps and hotspots over Balasore

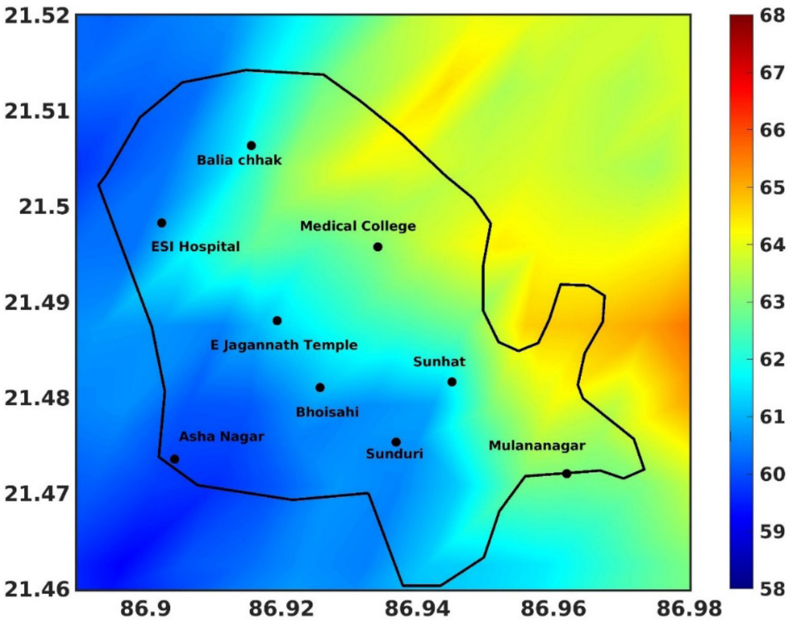

Fig. 10 Annual average concentration of $PM_{2.5}$ over Balasore

The annual map of $PM_{2.5}$ over Balasore shows that the North-Eastern parts have higher values ***(more than 60 µgm^{-3})***. In comparison, the southern and western regions have comparatively lower values (ranges between 58-62 µgm^{-3}). In addition, the particulate mass concentrations were higher in the periphery of the city (North-Eastern region) than the city itself. It needs to be investigated why such large gradients exist on a small spatial scale. However, it may be noted that it is not surprising that such gradients exist. The potential cause needs to be explored from scientific and policy perspectives to reduce particulate pollution levels. For example, there are several possible reasons for such concentration gradients, such as varying topography, microclimate and circulation pattern of the city, emission hotspots outside the city boundary etc.

The seasonal variation of $PM_{2.5}$ over Balasore (Fig. 11) shows that the north-eastern periphery area of the city experiences higher values in all the seasons. The winter season shows the highest loading ***(more than 80 µgm^{-3})*** followed by post-monsoon. The $PM_{2.5}$ is well distributed during monsoon.

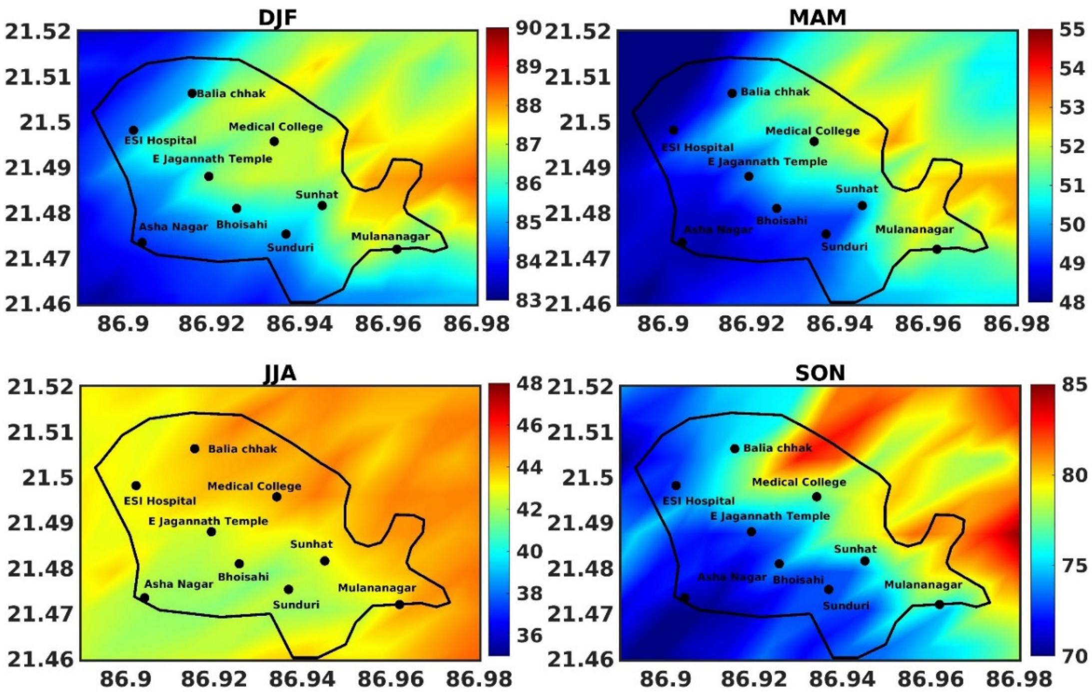

Fig. 11 Seasonal Concentration of $PM_{2.5}$ over Balasore

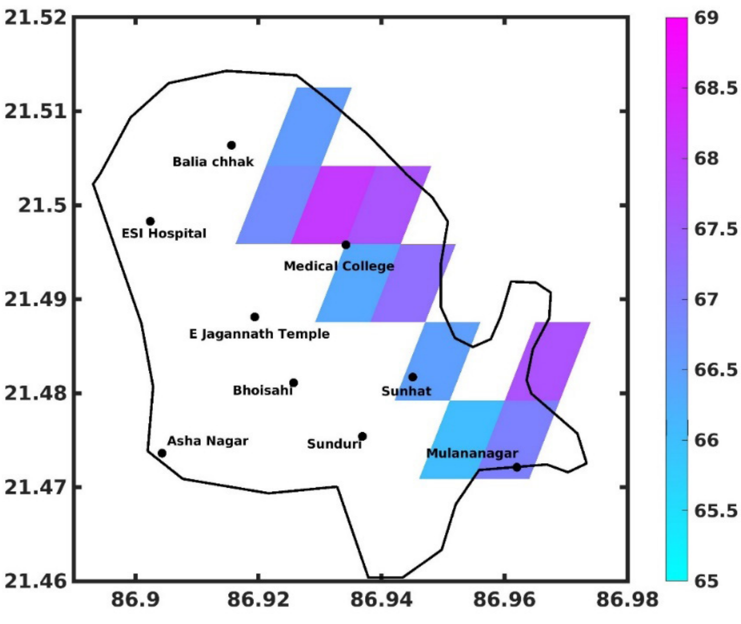

Fig. 12 Annual $PM_{2.5}$ hotspots over Balasore

The **figure 12** shows the annual $PM_{2.5}$ hotspots over Balasore. The 70 percentile data is ***more than 65 µgm^{-3}*** which is even much higher than industrial areas like Angul. It is to be noted that the whole eastern part of the city acts as continuous hotspots or experiences stagnation due to some reason. The hotspots identified in this study are,

i. 2 to 2.5 km area surrounding Medical College and Hospital.

ii. Area including Mulannagar, Sunhat and Old Balasore.

7.3 Annual and Seasonal $PM_{2.5}$ maps and Hotspots over Bhubaneswar

The **figure 13** shows the yearly average concentration of $PM_{2.5}$ over the Bhubaneswar region. It is seen that ***Chandrasekharpur and Mancheswar*** areas show the highest concentration levels. The annual average of the site is ***~60 µgm^{-3}***. Typically, the value of $PM_{2.5}$ in the urban area is much higher than in the surroundings like Patrapada. The areas near the Lingaraja Temple and Baramunda also show higher annual PM2.5 values.

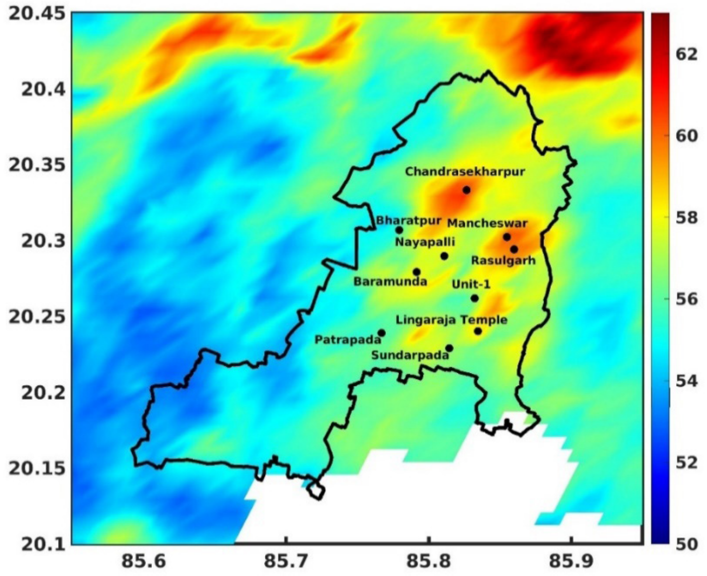

Fig. 13 Annual average concentration of $PM_{2.5}$ over Bhubaneswar. (Color bar indicates mass concentrations in µg m^{-3})

The **figure 14** shows the seasonal variation of $PM_{2.5}$ over Bhubaneswar. It appears that winter (DJF) ***(~75 µgm^{-3}***) and the post-monsoon (SON) ***(~68 µgm^{-3})*** periods experience high $PM_{2.5}$ loading compared to the other two seasons. Chandrasekharpur, Mancheswar, and Unit-1 show higher values in all the seasons. The northern part of the city shows higher concentration levels than the southern part. In addition, an exceptionally high concentration is also observed over the Chandaka forest area to the west of the town. It is not clear whether this is a pollution layer or retrieval error induced due to change in the land cover pattern or other unknown issues during the pre-monsoon period.

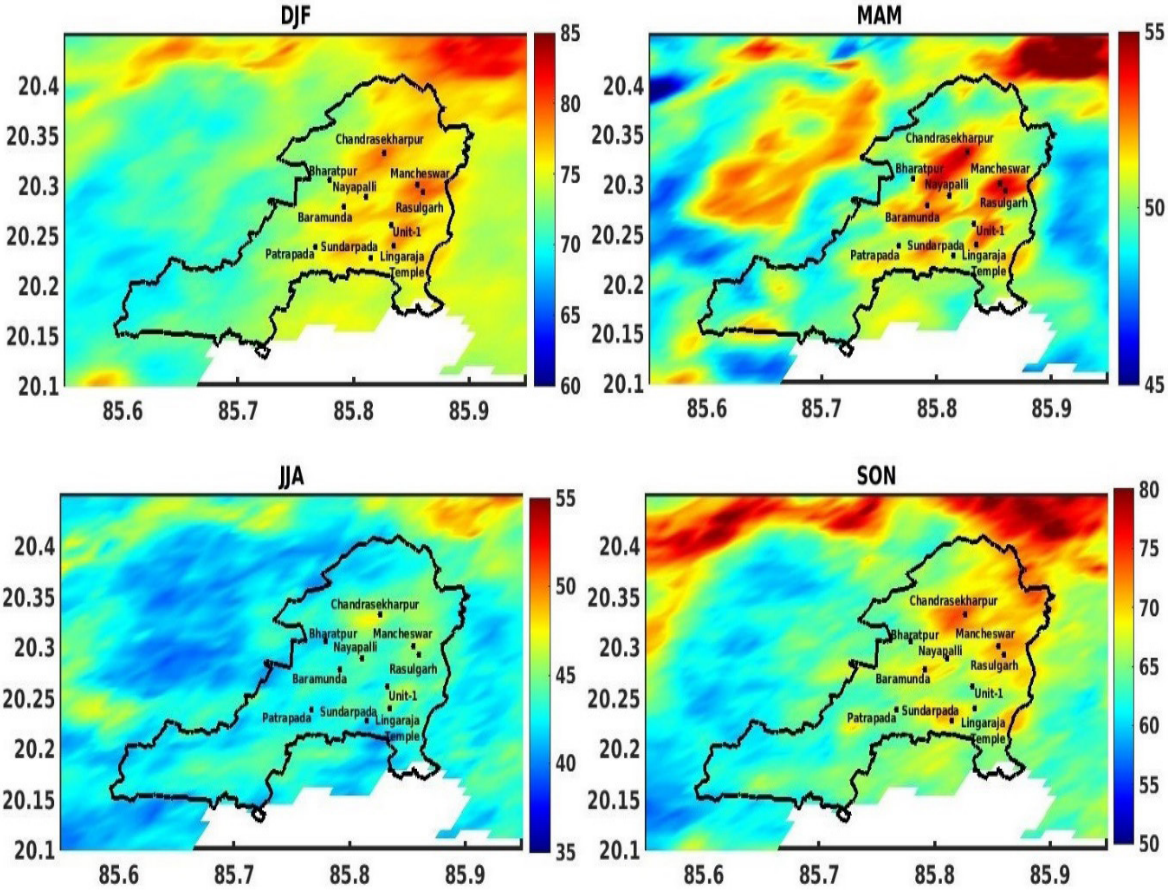

Fig. 14 Seasonal Concentration of $PM_{2.5}$ over Bhubaneswar.

The **figure 15** shows the $PM_{2.5}$ hotspots over Bhubaneswar. It is important to note that the values are ***higher than 57.28 µgm^{-3}***, representing the 70 percentile of the datasets used for this identification. The hotspots are identifiable during all seasons, such as winter and pre-and post-monsoon periods. From this analysis, the top 5 hotspots may be listed as,

i. Chandrasekharpur area.

ii. Mancheswar Industrial area.

iii. Lingaraja Temple area.

iv. Baramunda area.

v. Sundarpada area.

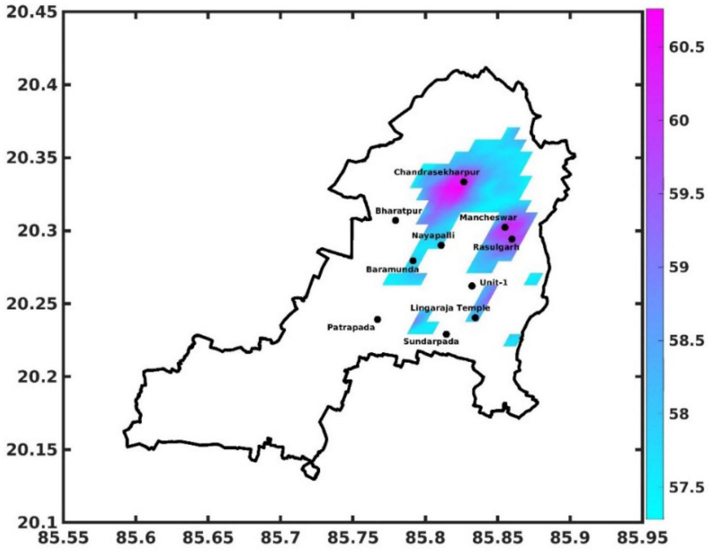

Fig. 15 Annual $PM_{2.5}$ hotspots over Bhubaneswar

7.4 Annual and Seasonal $PM_{2.5}$ maps and Hotspots over Cuttack

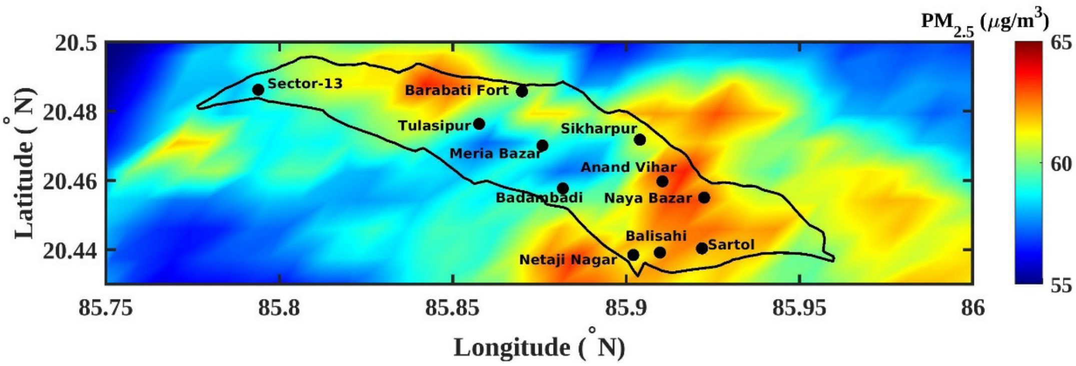

Fig. 16 Annual average concentration of $PM_{2.5}$ over Cuttack

The **figure 16** shows the yearly average $PM_{2.5}$ map over Cuttack city. The figure shows that the southern part of the city is more polluted than the northern part. The annual average of $PM_{2.5}$ over Cuttack is more than ***58 μgm⁻³*** which depicts high pollution loading over the city. Areas like ***Sikharpur, Anand Vihar, Naya Bazar, Balisahi, Sartol*** shows high $PM_{2.5}$ loading.

The **figure 17** shows the seasonal variation of $PM_{2.5}$ over Cuttack. The figure depicts that post-monsoon (SON) and winter season (DJF) experiences high $PM_{2.5}$ loading ***(more than 75 μgm⁻³)***. However, the high loading is more or less evenly distributed during the winter. Irrespective of seasons, the southern and eastern parts show higher values than the western. It is also observed that surfaces such as sand in the rivers are shown with higher $PM_{2.5}$ loading. This aspect need to be addressed in the future based on ground-based campaign. However, this may also be a consequence of the land type differences used in the aerosol retrieval from satellites.

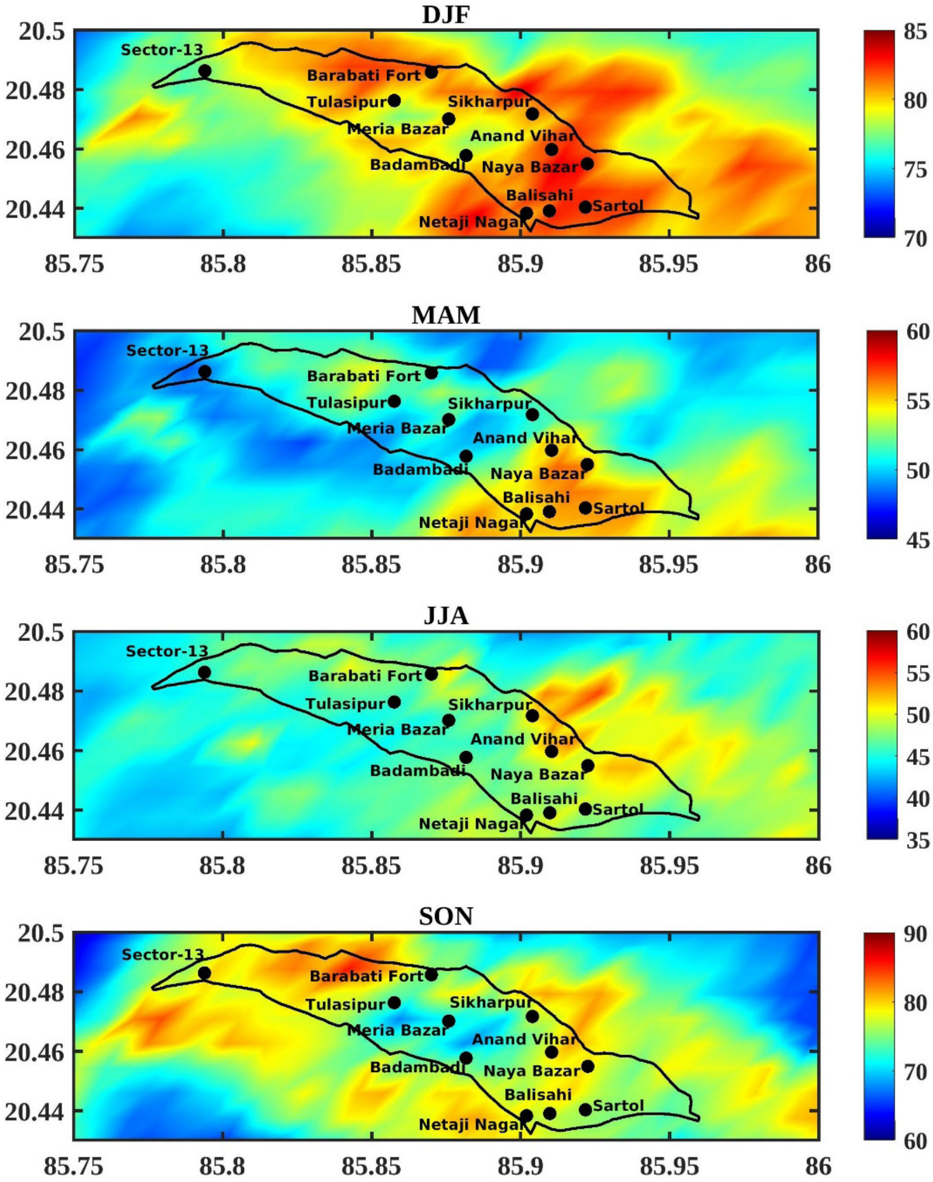

Fig. 17 Seasonal Concentration of $PM_{2.5}$ over Cuttack

The **figure 18** depicts the annual $PM_{2.5}$ hotspots over Cuttack. The 70^{th} percentile values are higher than ***64 μgm⁻³***, much **higher than Bhubaneswar**. The hotspots are well marked in all the seasons and can be identified as follows,

i. Barabati Stadium area.

ii. Sikharpur Area.

iii. Sartol Area

iv. Area including Anand Vihar and Naya Bazar

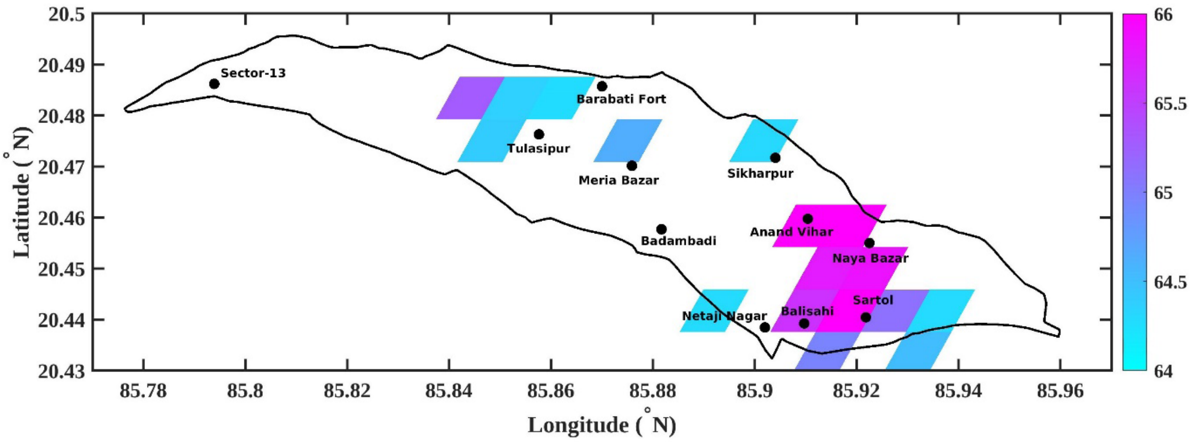

Fig. 18 Annual $PM_{2.5}$ hotspots over Cuttack

7.5 Annual and Seasonal $PM_{2.5}$ maps and Hotspots over Kalinganagar

The yearly average of $PM_{2.5}$ shows that the eastern part of the city has high $PM_{2.5}$ loading ***(more than 56 µgm^{-3})***. Areas near Gobra Ghati, Badasuli, VISA steel shows high $PM_{2.5}$ loading. On a seasonal time scale, the winter period shows high $PM_{2.5}$ loading followed by the post-monsoon period. The $PM_{2.5}$ ***values reach up to 90 µgm^{-3}***. Except for the monsoon, all other seasons depict high $PM_{2.5}$ loading over the city area. The city's eastern part shows higher values in all seasons except the post-monsoon period. The large air pollution gradient over this region requires ground-based campaigns to understand whether these spatial maps are consistent with the actual ground-level concentration levels. Such campaigns will provide the much-needed validation and trust in satellite mapping of ground-level pollution hotspots. The precise identification of hotspots during SON could be due to the large-scale rainfall that may have enhanced the local emissions over this town. Overall, the western and central part of the town appears to be a hotspot affected by particulate matter pollution. It will be interesting to explore whether this is a consequence of the city emissions or those transported from nearby industrial units.

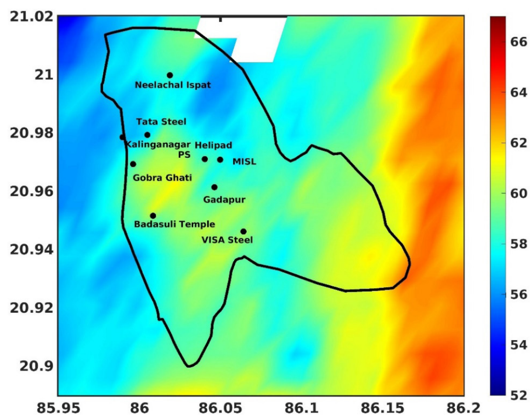

Fig. 19 Annual average concentration of $PM_{2.5}$ over Kalinganagar

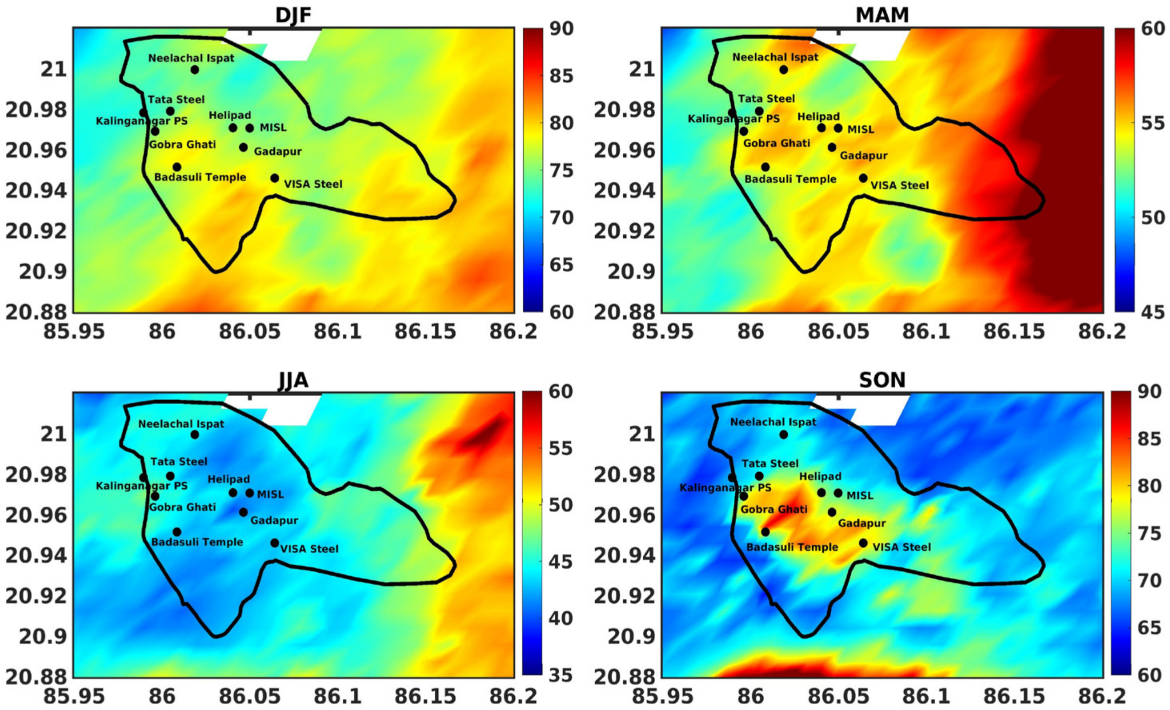

Fig. 20 Seasonal Concentration of $PM_{2.5}$ over Kalinganagar

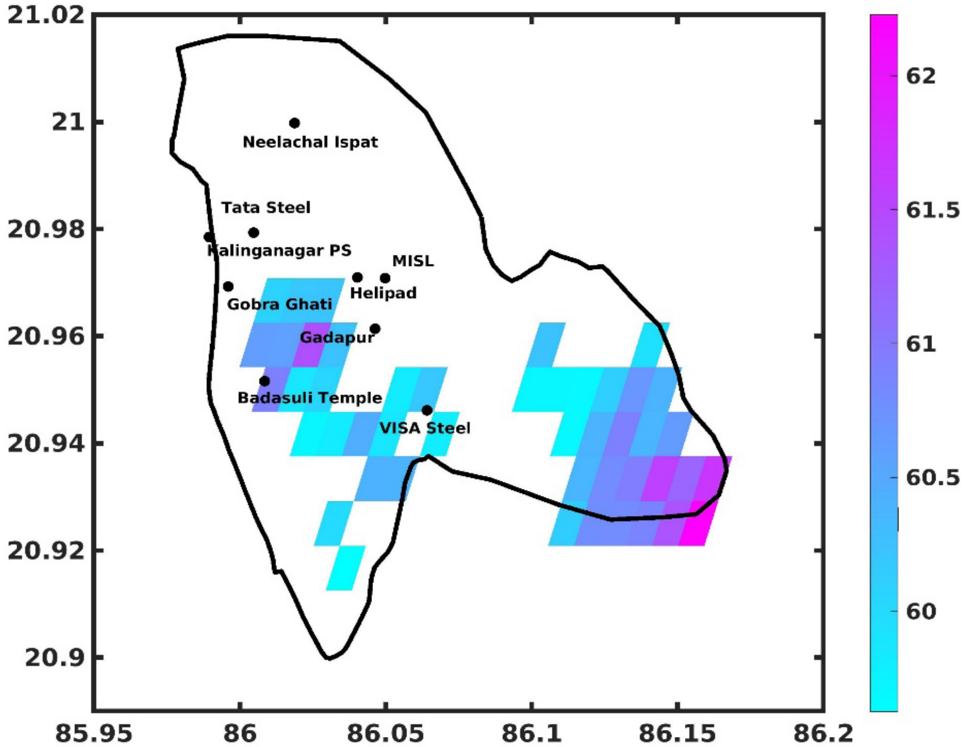

Fig. 21 Annual $PM_{2.5}$ hotspots over Kalinganagar

The $PM_{2.5}$ hotspots over Kalinganagar can be listed as,

i. Southern part of Kalinganagar Industrial Area.

ii. Area surrounding F.C colony.

7.6 Annual and Seasonal $PM_{2.5}$ maps and Hotspots over Rourkela

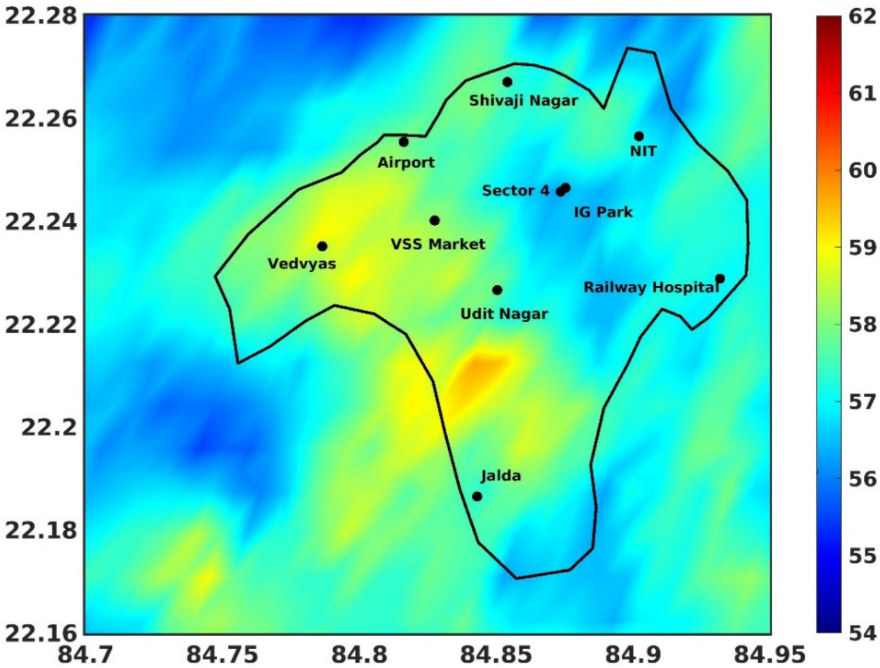

Fig. 22 Annual average concentration of $PM_{2.5}$ over Rourkela

The yearly map of $PM_{2.5}$ over Rourkela shows that the western (both central and south in Fig. 22) part of the city experiences high loading ***(more than 58 µgm^{-3})***. Areas like the VSS market, Vedvyas, Airport Udit Nagar indicate higher $PM_{2.5}$ loading. However, areas like NIT, Shivaji Nagar show comparatively lower $PM_{2.5}$ loading.

Figure 23 depicts the seasonal variation of $PM_{2.5}$ over Rourkela. The winter period shows high $PM_{2.5}$ loading ***(more than 68 µgm^{-3})*** followed by the post-monsoon period. The high loading areas shifted to the northern part during the monsoon. Significant variability in $PM_{2.5}$ loading can be observed seasonally. However, the loading is evenly distributed in post-monsoon (SON). The existence of a hotspot irrespective of the season is one potentially best method to identify potential emission sources.

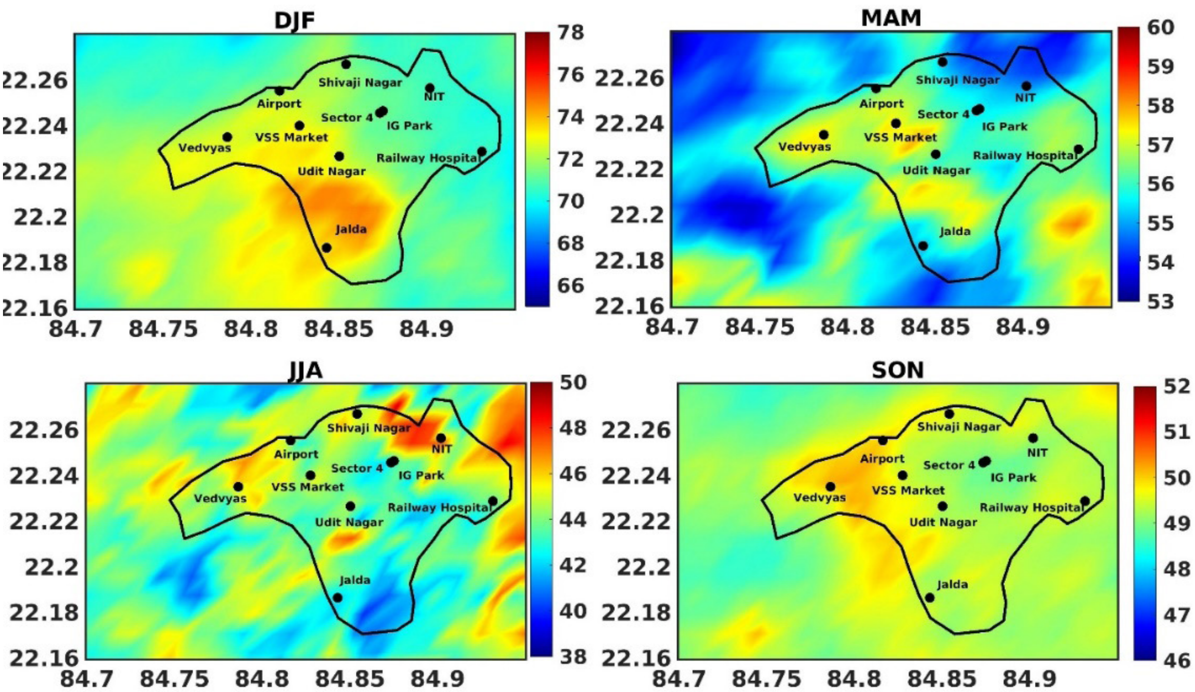

Fig. 23 Seasonal Concentration of $PM_{2.5}$ over Rourkela

The $PM_{2.5}$ hotspot areas over Rourkela (Fig. 28) can be listed as,

i. Chhend Colony, Vedvyas and Udit Nagar area .

ii. Rourkela Steel Plant area.

iii. Jalda and Deoga Area.

iv. Kuarmunda Area.

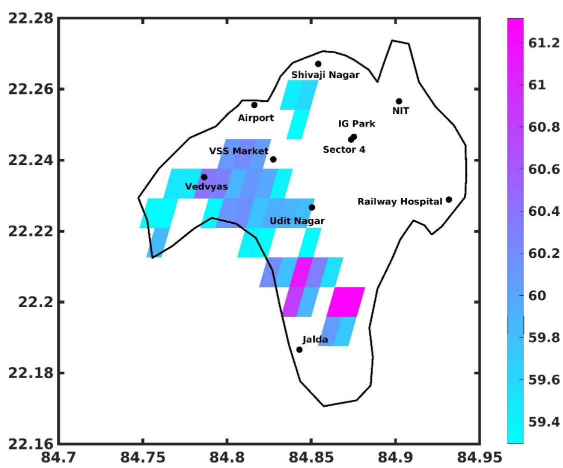

Fig. 24 Annual $PM_{2.5}$ hotspots over Rourkela

7.7 Annual and seasonal $PM_{2.5}$ maps and Hotspots over Talcher

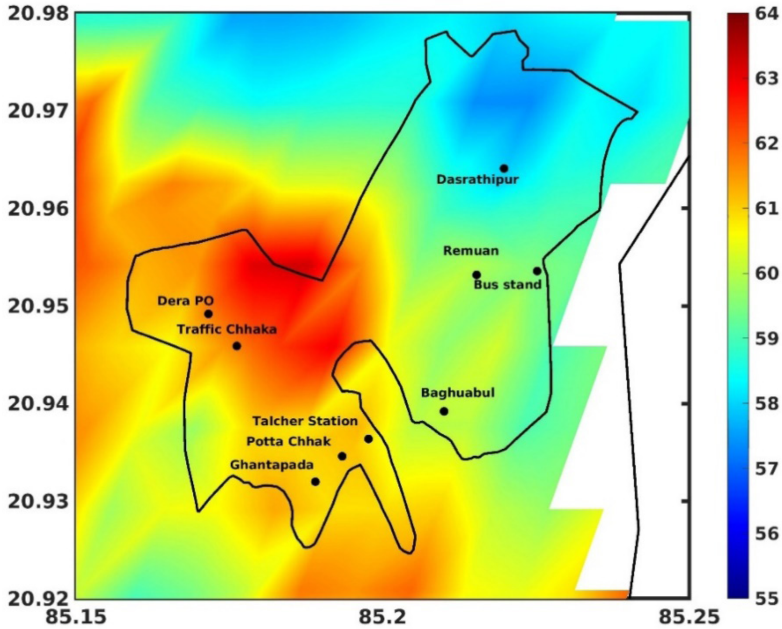

Fig. 25 Annual average concentration of $PM_{2.5}$ over Talcher

The yearly average of $PM_{2.5}$ is significantly high over the Talcher town ***(more than 58 µgm⁻³)***. The western part of the town shows higher values than the eastern part. Areas like Dera PO, Traffic Chhaka Potta Chhak, Ghantapada, etc., indicate higher $PM_{2.5}$ loading.

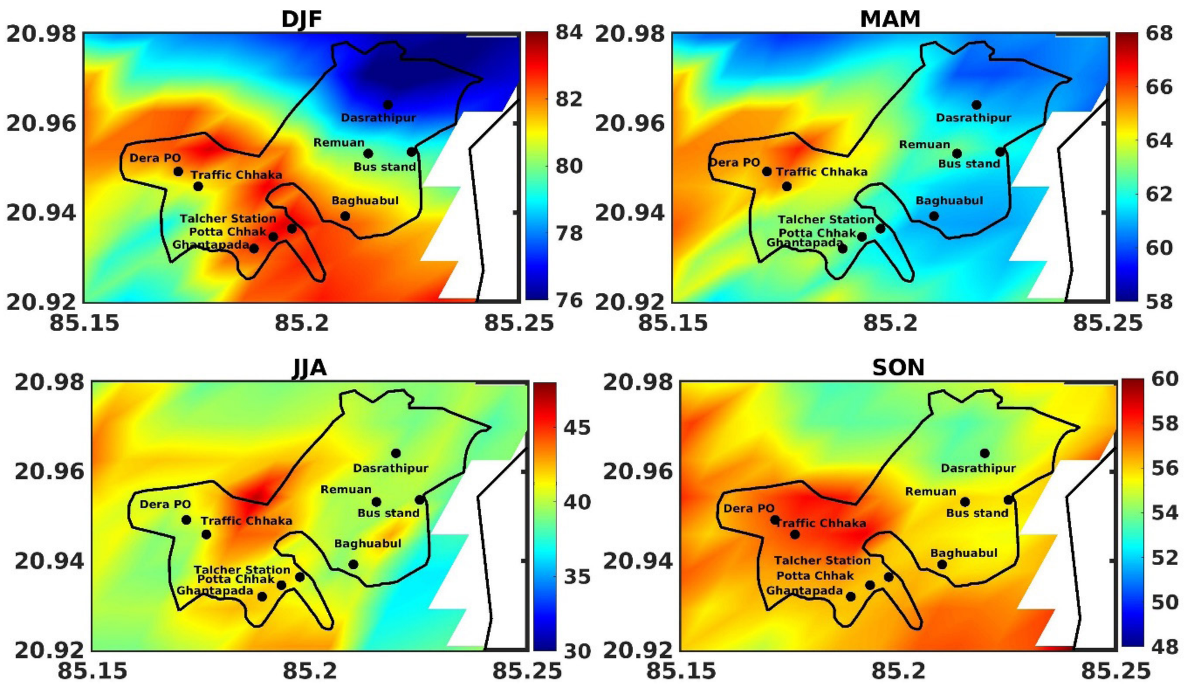

Fig. 26 Seasonal Concentration of $PM_{2.5}$ over Talcher

The seasonal variation of the $PM_{2.5}$ loading over Talcher shows that the winter ***(more than 75 μgm^{-3})*** period experiences high PM2.5 loading followed by the pre-monsoon. A clear north-south gradient can be observed with a northern low and southern high in all seasons. The traffic Chhaka near Dera PO along with any potential emission sources, maybe a particulate emission source for this region.

The 70 percentile data over Talcher (Fig. 27) is more than ***66 μgm^{-3}*** which is much higher than Bhubaneswar, Angul, and Cuttack. The hotspots can be listed as,

i. Dera Chhaka and surrounding area.

ii. Bypass Chhaka including Talcher Station and Ghantapada.

iii. Baghuabul area.

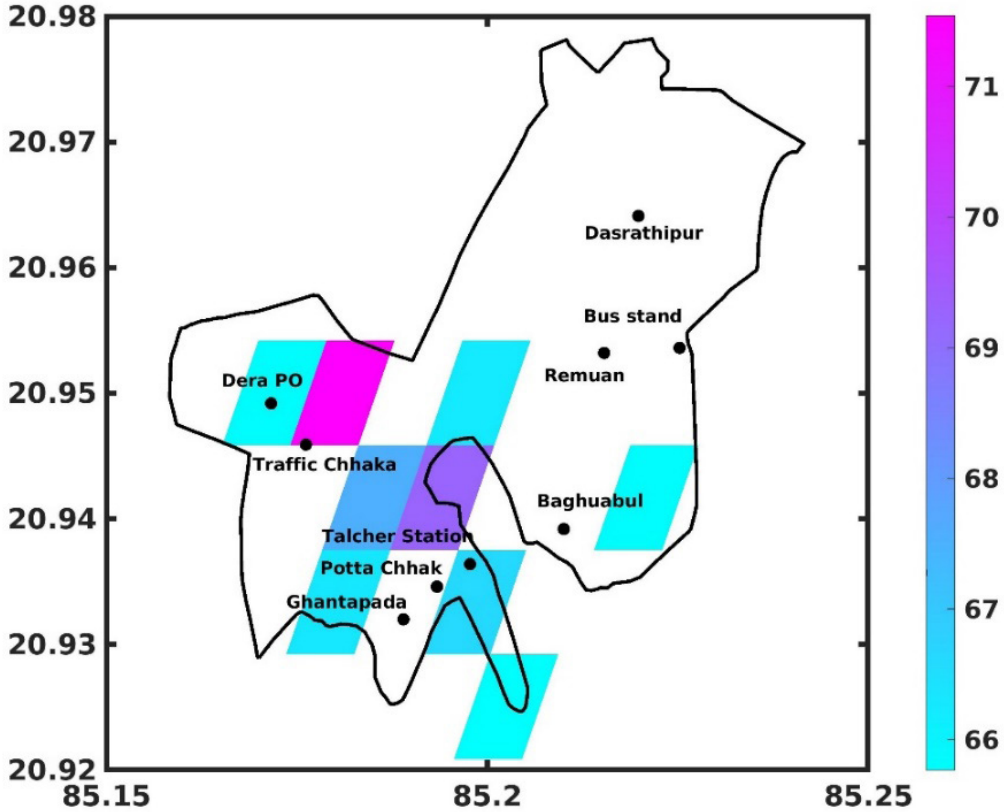

Fig. 27 Annual $PM_{2.5}$ hotspots over Talcher

7.8 Combined Hotspots

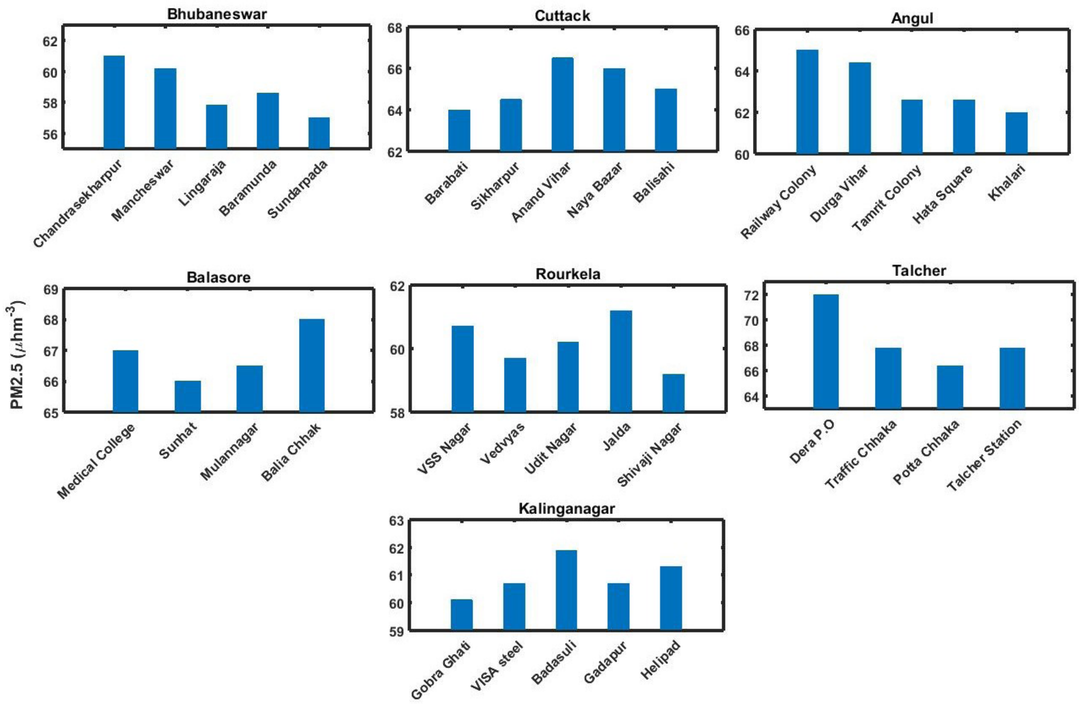

Fig. 28 Hotspots and their respective $PM_{2.5}$ concentrations over the Non-attainment cities based on the M-S method. Note the independent y-axis properties to allow for selected city level hotspots and their comparison.

Finally, **figure 28** provides a glimpse of all the annual hotspots over the non-attainment cities. It is to be noted that the base concentration of $PM_{2.5}$ over all the hotspots is higher than their 70 percentile data, respectively indicating that most of the sites studied have air pollution or particulate concentration levels higher than the standards prescribed by CPCB. In addition, hotspots over smaller regions/towns such as Talcher and Balasore show higher $PM_{2.5}$ concentrations than those over Bhubaneswar. It may be noted that such inter-comparisons need to be made cautiously as this method of $PM_{2.5}$ is not constrained by surface measurements and need to be validated. However, hotspot comparisons within the cities are reasonable and may be used to make policy-level decisions. Overall, it is requested that a thorough ground campaign be made at each of these cities so as to obtain ground truth and validate these findings.

8. Results and Discussion (G-S Method)

The current analysis presents the $PM_{2.5}$ maps and hotspots generated using the Ground-Satellite method or the G-S method.

8.1 Annual and Seasonal $PM_{2.5}$ maps and Hotspots over Bhubaneswar (G-S Method)

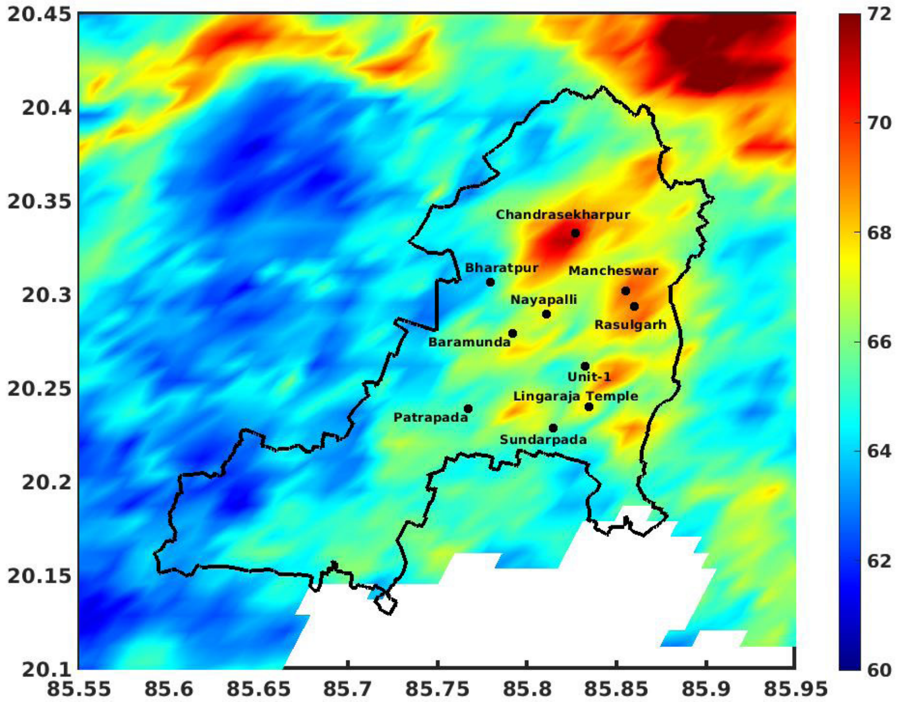

Fig. 29 Annual average concentration of $PM_{2.5}$ over Bhubaneswar (G-S Method)

The **figure 29** depicts the annual average concentration of $PM_{2.5}$ over Bhubaneswar using the G-S method. It appears that the G-S method estimated higher $PM_{2.5}$ values than the M-S method. However, the spatial distribution pattern of $PM_{2.5}$ is similar in both cases. The higher value regions like Chandrasekharpur and Mancheswar also appear in the maps generated using the G-S method.

The **figure 30** shows the seasonal maps of $PM_{2.5}$ using the G-S method. It appears that the winter (DJF) and pre-monsoon (MAM) values are higher in this method. On the other hand, the post-monsoon (SON) $PM_{2.5}$ loading is lower than the M-S method. However, the spatial patterns and hence the hotspots appear to be comparable.

Finally, figure 38 depicts the $PM_{2.5}$ hotspots using the G-S method. The threshold value is higher ***(~64 µgm^{-3})*** than the M-S method. However, similar hotspots can be identified. The similarity confirms the consistency of the technique over the study area. It appears that the use of ground-based observational data improves the derived $PM_{2.5}$ values.

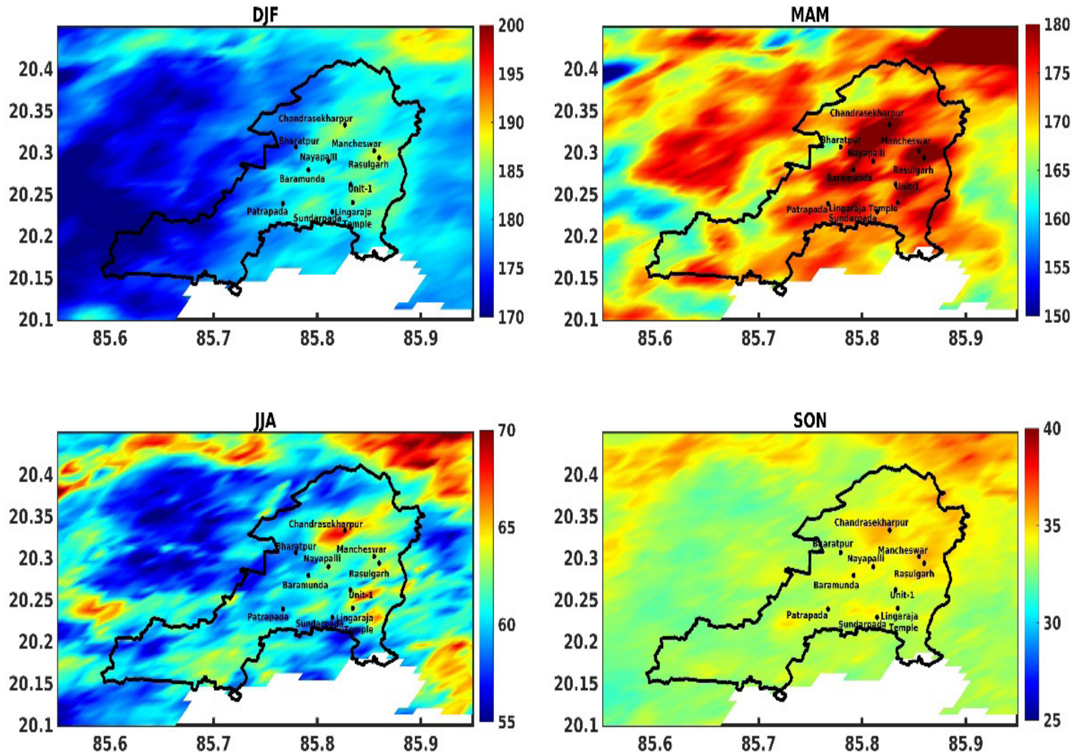

Fig. 30 Seasonal Concentration of $PM_{2.5}$ over Bhubaneswar (G-S Method). (Difference in color bar used for different periods to highlight the hotspots)

The $PM_{2.5}$ values for the other cities derived using the G-S method are abnormally high biased and hence not discussed in this report. It is to be mentioned that the G-S method primarily depends on the temporal and spatial resolution of the $PM_{2.5}$, RH, and PBLH data. Therefore, the absence of continuous observational $PM_{2.5}$ data, high-resolution RH, and PBLH values can introduce profound errors to the equations generated for these cities, producing such high $PM_{2.5}$ values.

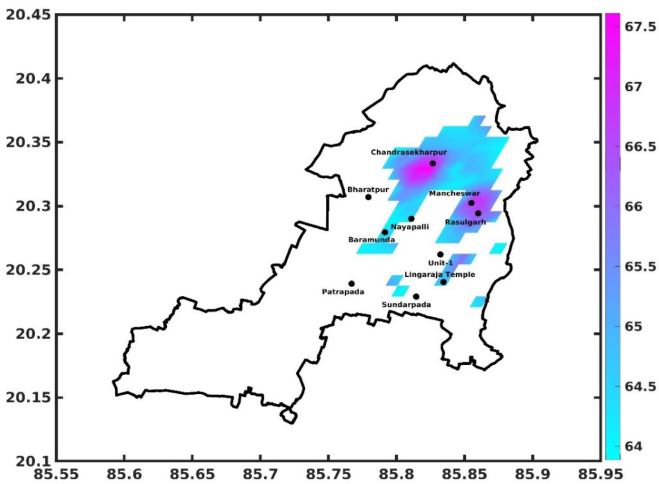

Fig. 31 Annual $PM_{2.5}$ hotspots over Bhubaneswar (G-S Method)

8.2 Bias Correction

The present section shows the inter-comparison between the derived and observed $PM_{2.5}$. The values generated using the M-S method are utilized for the corrections. Bias correction techniques are applied to calculate the bias in different temporal scales. Finally, the observed and bias-corrected data are compared, and statistical analysis is performed. The mean bias correction method has been applied in three different scales (annual, monthly, and seasonal).

$$\mathbf{B_i = \bar{X} - \bar{Y}} \tag{3}$$

Where, $\bar{X}$ is the observed $PM_{2.5}$ data and $\bar{Y}$ is the derived $PM_{2.5}$. B_i represents the mean difference. The bias-corrected $PM_{2.5}$ is described as,

$$\mathbf{PM_{2.5est} = \bar{Y} + B_i} \tag{4}$$

The **figure 32** shows the interrelation between observed and estimated data (without bias correction). It is evident that except for Talcher, all the cities show high bias. Several factors like rescaling of the MERRA data and lack of observational data can introduce errors to the derived relationships, generating such high $PM_{2.5}$ estimates. Therefore, only annual, seasonal and monthly bias correction is performed on the estimated $PM_{2.5}$ using equations (3) and (4). The **figure 33** shows that the yearly bias-corrected data compares better with the observed data. The lowest RMSE can be observed over Bhubaneswar, followed by Rourkela and Cuttack. This may also indicate the quality of satellite-based retrieval and the fidelity of the ground-level datasets used in the current analysis.

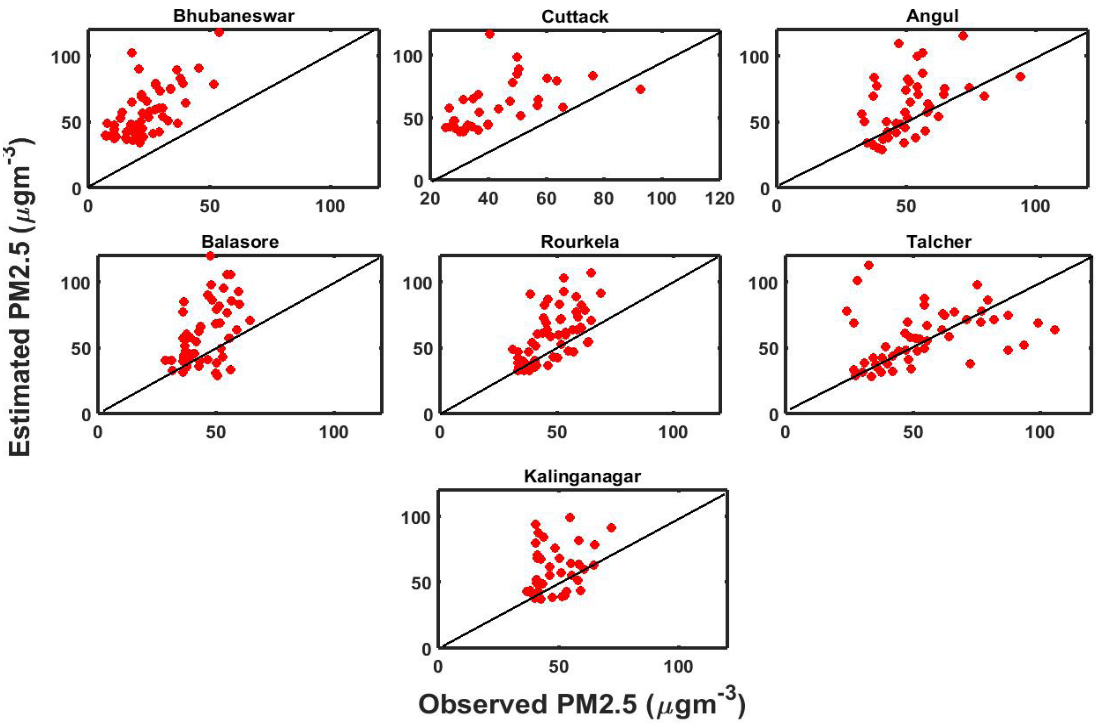

Fig. 32 Observed vs. Estimated $PM_{2.5}$ (without bias correction) over the non-attainment cities

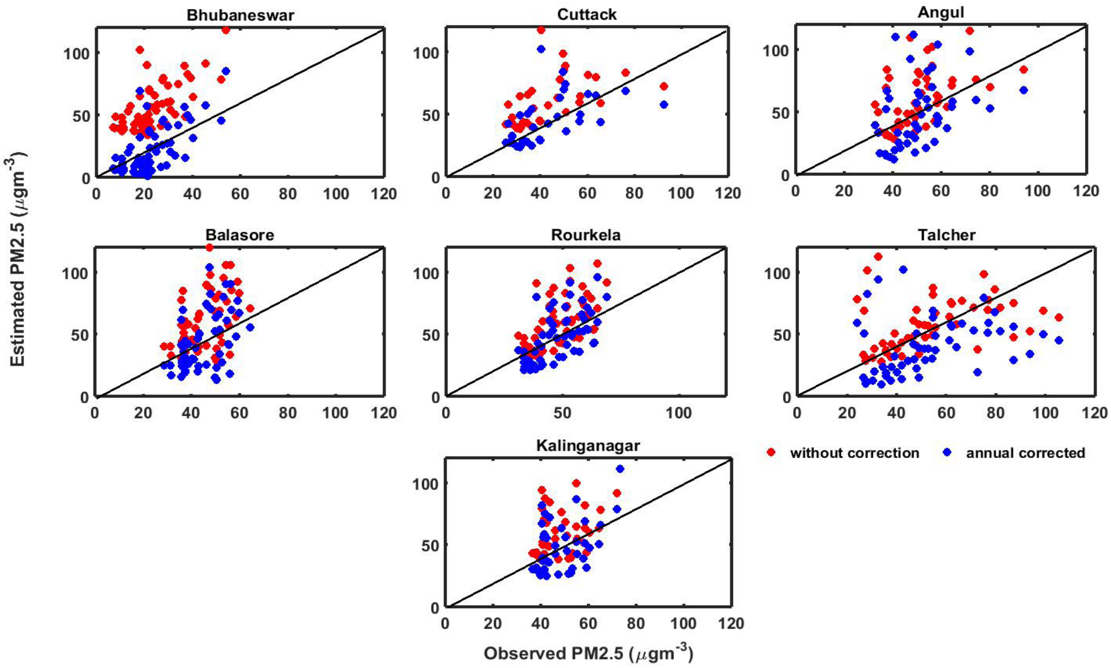

Fig. 33 Observed vs. Estimated $PM_{2.5}$ (Annual bias correction) over the non-attainment cities

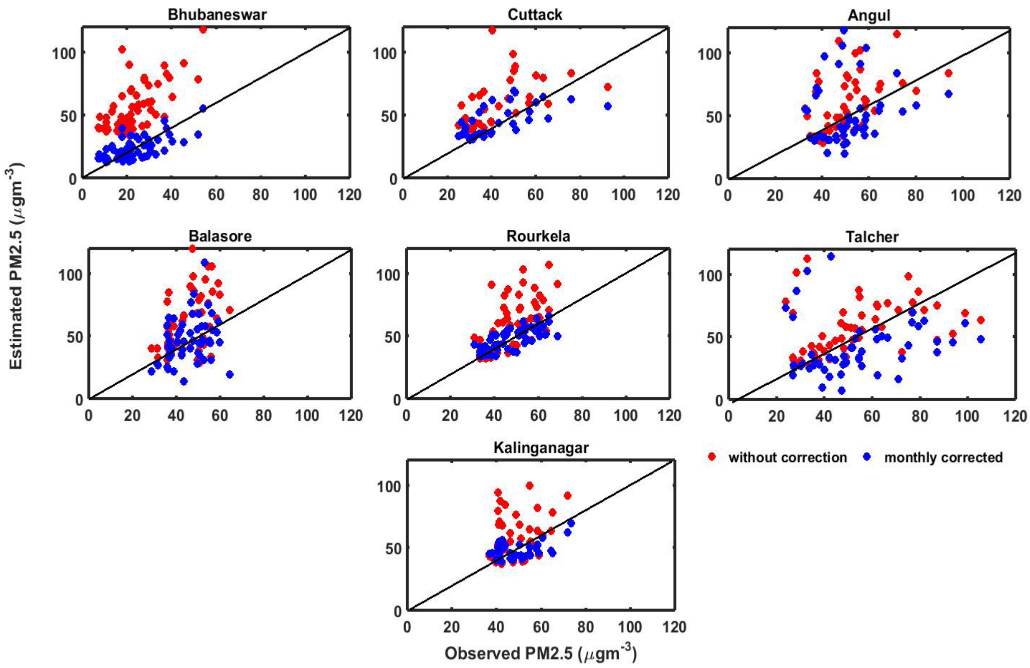

Fig. 34 Observed vs. Estimated $PM_{2.5}$ (Monthly bias correction) over the non-attainment cities

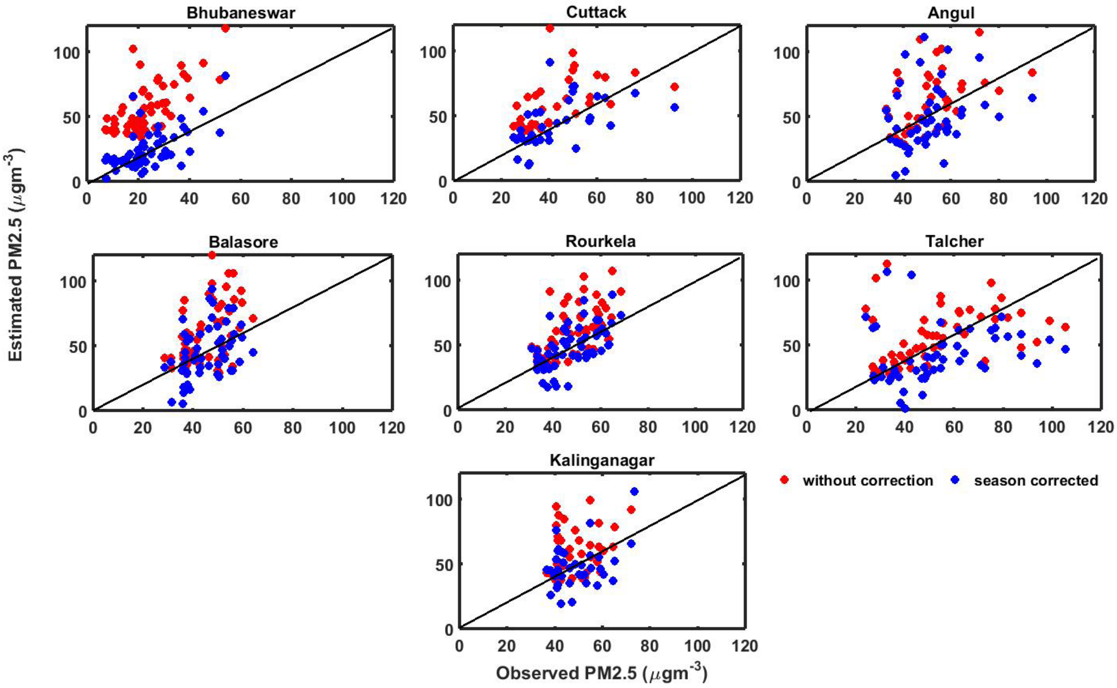

Fig. 35 Observed vs. Estimated $PM_{2.5}$ (Seasonal bias correction) over the non-attainment cities

The **figures 34 and 35** show the monthly and seasonal bias corrections, respectively. Table 1 shows that monthly bias correction shows lower RMSE and higher correlation than the annual and seasonal corrections. It has to be mentioned that Talcher always shows higher RMSE compared to the other stations. The reason behind such high RMSE needs to be investigated. Rourkela shows the lowest RMSE and highest correlation in the monthly and seasonal analysis. It has to be mentioned that the correlation between observed and estimated data over all the cities (except Talcher) is statistically significant, which shows the effectiveness of our estimation methods.

Table 1. Statistics of the bias correction

Station Name		Bhubaneswar	Cuttack	Angul	Balasore	Rourkela	Talcher	Kalinganagar
RMSE ($\mu g\ m^{-3}$)	Annual	**14.15**	17.06	**29.15**	23.85	**15.32**	**47.96**	18.08
	Monthly	**8.11***	12.15	**24.43**	16.85	**6.82***	**45.35**	8.73
	Seasonal	**12.64**	16.13	**27.34**	21.07	**12.72**	**46.61**	15.07
r	Annual	0.67	0.54	0.29	0.44	0.63	0.14	0.44
	Monthly	0.66	0.64	0.18	0.31	0.75	0.12	0.46
	Seasonal	0.59	0.54	0.22	0.40	0.60	0.16	0.37
r^2	Annual	0.45	0.30	0.08	0.19	0.40	0.02	0.19
	Monthly	0.43	0.41	0.03	0.10	0.56	0.01	0.22
	Seasonal	0.35	0.29	0.05	0.16	0.36	0.02	0.14

*Bhubaneswar and Rourkela datasets matched reasonably well with the satellite estimates.

9. Limitations of the Study

The results discussed in this report are primarily based on relationships between satellite AOD, and either model or surface-based $PM_{2.5}$ datasets by constraining meteorological factors. Therefore, the accuracy of the estimated surface $PM_{2.5}$ depends on the inputs used in deriving these relationships. The sources of error are thus the following,

1. AOD from the satellite is prone to systematic retrieval errors that vary in space and time. Thus, satellite AOD should first be validated against surface measurements, and their biases corrected. This is important specifically over locations/sites where apriori PM2.5 datasets are unavailable as there may not be a possibility to correct AOD biases that may influence the estimated $PM_{2.5}$.

2. AOD is affected by the vertical distribution of aerosols within the whole column of the atmosphere. However, PM2.5 is only a subset of this close to the surface of the Earth. Therefore, regions affected by long-range transport of aerosols may require a highly dynamic model that also considers such intermittent transport processes. Past studies have shown such long-range transport over coastal stations in Eastern India.

3. Many of the stations on the present study have proximity to Ocean and hence have high humidity. Therefore, the aerosol humidification effect modulates AOD-PM relationships and thus induces errors.

4. The lack of PM2.5 datasets with sufficient temporal frequency has allowed estimates only on seasonal and annual time scales in the present study. Estimates at daily time scales will require multiple stations to monitor continuous air quality at a temporal resolution of an hour or less.

Thus, the PM estimates made using different methods in this study need to be validated with ground and field surveys to understand their accuracy and biases.

10. Summary

The results obtained from the hotspot identification project are summarised below,

1. Both the methods (one using model (M-S method) and the other using surface measurements (G-S method)) show good promise in identifying air pollution hotspots over all the non-attainment cities over Odisha.

2. All the non-attainment cities had high $PM_{2.5}$ mass loading, much above the standards (60 ugm^{-3}), especially during the post-monsoon and winter seasons.

3. A total of 23 polluted localities were identified over the seven non-attainment cities.

   The details are as follows,

   a. Angul (*Area surrounding Railway Colony and Ranigoda, Tamrit Colony and adjoining Industrial Estate, Area surrounding Hari-Mohari Chhaka)*
   b. Balaosre *(2-2.5 km area surrounding Medical College and Hospital, Area including Mulannagar, Sunhat and Old Balasore)*
   c. Bhubaneswar (*Chandrasekharpur area, Mancheswar Industrial area, Lingaraj Temple area, Baramunda area, Sundarpada area)*
   d. Cuttack (*Barabati Stadium area, Sikharpur area, Area including Anand Vihar, NayaBazar and Balisahi)*
   e. Kalinganagar (*Southern part of Kalinganagar Industrial Estate, Area Surrounding F.C colony)*
   f. Rourkela (*Chhend Colony, Vedvyas and Udit Nagar area, Rourkela Steel Plant area, Jalda and Deoga area, Kuamunda area)*
   g. Talcher (*Dera Chhaka and surrounding area, Bypass Chhaka including Talcher Station and Ghantapada, Baghuabul area)*

There may be other more polluted localities outside the city limits. The focus of the study was primarily on localities within the different cities considered in this work.

4. Major hotspots could be identified in all the cities. In most of these hotspots, the annual $PM_{2.5}$ concentrations is higher than 60 $\mu gm^{-3,}$ which is a major concern.

Future research may focus on validating the results obtained in this analysis using high-resolution field measurements and surveys. In addition, model-based exploration may also be attempted to obtain higher resolution mapping of PM2.5 in cities that have high-resolution emission inventory information. This will enable the potential for mitigation efforts to reduce air pollution at the city scale. If emission inventories are lacking, satellite measurements along with simulations could be used to obtain a realistic spatio-temporal distribution of PM2.5 for quick policy efforts.

References

Atwater, M. A. (1970). Planetary albedo changes due to aerosols. *Science* 170, 64–6. doi:10.1126/science.170.3953.64.

Beegum, S. N., Moorthy, K. K., and Babu, S. S. (2009). Aerosol microphysics over a tropical coastal station inferred from the spectral dependence of Angstrom wavelength exponent and inversion of spectral aerosol optical depths. *J. Atmos. Solar-Terrestrial Phys.* 71, 1846–1857. doi:10.1016/j.jastp.2009.07.004.

Brauer, M., Amann, M., Burnett, R. T., Cohen, A., Dentener, F., Ezzati, M., et al. (2012). Exposure assessment for estimation of the global burden of disease attributable to outdoor air pollution. *Env. Sci Technol* 46, 652–60. doi:10.1021/es2025752.Exposure.

Brook, R. D., Rajagopalan, S., Pope, C. A., Brook, J. R., Bhatnagar, A., Diez-Roux, A. V., et al. (2010). Particulate matter air pollution and cardiovascular disease: An update to the scientific statement from the american heart association. *Circulation* 121, 2331–2378. doi:10.1161/CIR.0b013e3181dbece1.

Chowdhury, S., and Dey, S. (2016). Cause-specific premature death from ambient PM2.5exposure in India: Estimate adjusted for baseline mortality. *Environ. Int.* 91, 283–290. doi:10.1016/j.envint.2016.03.004.

Chowdhury, S., Dey, S., and Smith, K. R. (2018). Ambient PM2.5 exposure and expected premature mortality to 2100 in India under climate change scenarios. *Nat. Commun.* 9, 318. doi:10.1038/s41467-017-02755-y.

Dey, S., Tripathi, S. N., Singh, R. P., and Holben, B. N. (2005). Seasonal variability of the aerosol parameters over Kanpur, an urban site in Indo-Gangetic basin. *Adv. Sp. Res.* 36, 778–782. doi:10.1016/j.asr.2005.06.040.

Dipu, S., Prabha, T. V., Pandithurai, G., Dudhia, J., Pfister, G., Rajesh, K., et al. (2013). Impact of elevated aerosol layer on the cloud macrophysical properties prior to monsoon onset. *Atmos. Environ.* 70, 454–467. doi:10.1016/J.ATMOSENV.2012.12.036.

Dockery, D. W. (2014). Health Effects of Particulate Air Pollution. *Ann. Epidemiol.* 19, 1–49. doi:10.1016/j.annepidem.2009.01.018.

Ensor, D. S., Porch, W. M., Pilat, M. J., Charlson, R. J., Ensor, D. S., Porch, W. M., et al. (1971). Influence of the Atmospheric Aerosol on Albedo. *J. Appl. Meteorol.* 10, 1303–1306. doi:10.1175/1520-0450(1971)010<1303:IOTAAO>2.0.CO;2.

Gu, Y., Liou, K. N., Jiang, J. H., Su, H., and Liu, X. (2012). Dust aerosol impact on North Africa climate: a GCM investigation of aerosol-cloud-radiation interactions using A-Train satellite data. *Atmos. Chem. Phys.* 12, 1667–1679. doi:10.5194/acp-12-1667-2012.

Han, Y., Wu, Y., Wang, T., Zhuang, B., Li, S., and Zhao, K. (2015). Impacts of elevated-aerosol-layer and aerosol type on the correlation of AOD and particulate matter with ground-based and satellite measurements in Nanjing, southeast China. *Sci. Total Environ.* 532, 195–207. doi:10.1016/j.scitotenv.2015.05.136.

Hoek, G., Krishnan, R. M., Beelen, R., Peters, A., Ostro, B., Brunekreef, B., et al. (2013). Long-term air pollution exposure and cardio-respiratory mortality: A review. *Environ. Heal. A Glob. Access Sci. Source* 12. doi:10.1186/1476-069X-12-43.

Krishna Moorthy, K., Suresh Babu, S., Manoj, M. R., and Satheesh, S. K. (2013). Buildup of aerosols over the Indian Region. *Geophys. Res. Lett.* 40. doi:10.1002/grl.50165.

Lee, H. J., Liu, Y., Coull, B. A., Schwartz, J., and Koutrakis, P. (2011). A novel calibration approach of MODIS AOD data to predict PM2.5 concentrations. *Atmos. Chem. Phys.* 11, 7991–8002. doi:10.5194/acp-11-7991-2011.

Li, J., Carlson, B. E., and Lacis, A. A. (2015). How well do satellite AOD observations represent the spatial and temporal variability of PM2.5 concentration for the United States? *Atmos. Environ.* 102, 260–273. doi:10.1016/j.atmosenv.2014.12.010.

Lim, S. S., Vos, T., Flaxman, A. D., Danaei, G., Shibuya, K., Adair-Rohani, H., et al. (2012). A comparative risk assessment of burden of disease and injury attributable to 67 risk factors and risk factor clusters in 21 regions, 1990–2010: a systematic analysis for the Global Burden of Disease Study 2010. *Lancet* 380, 2224–2260. doi:10.1016/S0140-6736(12)61766-8.A.

Liu, Y., Franklin, M., Kahn, R., and Koutrakis, P. (2007). Using aerosol optical thickness to predict ground-level PM2.5 concentrations in the St. Louis area: A comparison between MISR and MODIS. *Remote Sens. Environ.* 107, 33–44. doi:10.1016/j.rse.2006.05.022.

Liu, Y., Park, R. J., Jacob, D. J., Li, Q., Kilaru, V., and Sarnat, J. A. (2004). Mapping annual mean ground-level PM2.5 concentrations using Multiangle Imaging Spectroradiometer aerosol optical thickness over the contiguous United States. *J. Geophys. Res. D Atmos.* 109, 1–10. doi:10.1029/2004JD005025.

Lohmann, U., and Feichter, J. (2004). Global indirect aerosol effects: a review. *Atmos. Chem. Phys. Discuss.* 4, 7561–7614. doi:10.5194/acpd-4-7561-2004.

Menon, S., Hansen, J., Nazarenko, L., and Luo, Y. (2002). Climate effects of black carbon aerosols in China and India. *Science (80-.).* 297, 2250–2253. doi:10.1126/science.1075159.

Mukherjee, T., and Vinoj, V. (2020). Atmospheric aerosol optical depth and its variability over an urban location in Eastern India. *Nat. Hazards* 102, 591–605. doi:10.1007/s11069-019-03636-x.

Navinya, C. D., Vinoj, V., and Pandey, S. K. (2020). Evaluation of PM2.5 Surface Concentrations Simulated by NASA's MERRA Version 2 Aerosol Reanalysis over India and its Relation to the Air Quality Index. *Aerosol Air Qual. Res.*, 1329–1339. doi:10.4209/aaqr.2019.12.0615.

Ning, H., Li-juan, L., and Bin, W. (2015). The Role of the Aerosol Indirect Effect in the Northern Indian Ocean Warming Simulated by CMIP5 Models. *Atmos. Ocean. Sci. Lett.* 2834, 411–416. doi:10.3878/j.issn.1674-2834.14.0032.

Paciorek, C. J., Liu, Y., Moreno-Macias, H., and Kondragunta, S. (2008). Spatiotemporal associations between GOES aerosol optical depth retrievals and ground-level PM2.5.

Environ. Sci. Technol. 42, 5800–5806. doi:10.1021/es703181j.

Pope III, C. A., Burnett, R. T., Thun, M. J., Calle, E. E., Krewski, D., and Thurston, G. D. (2002). Lung Cancer, Cardiopulmonary Mortality, and Long-term Exposure to Fine Particulate Air Pollution. *J. Am. Med. Assoc.* 287, 1132–1141. doi:10.1001/jama.287.9.1132.

Soni, M., Payra, S., and Verma, S. (2018). Particulate matter estimation over a semi arid region Jaipur, India using satellite AOD and meteorological parameters. *Atmos. Pollut. Res.* 9, 949–958. doi:10.1016/j.apr.2018.03.001.

Takemura, T., Nozawa, T., Emori, S., Nakajima, T. Y., and Nakajima, T. (2005). Simulation of climate response to aerosol direct and indirect effects with aerosol transport-radiation model. *J. Geophys. Res. D Atmos.* 110, 1–16. doi:10.1029/2004JD005029.

Tiwari, S., Hopke, P. K., Pipal, A. S., Srivastava, A. K., Bisht, D. S., Tiwari, S., et al. (2015). Intra-urban variability of particulate matter (PM2.5 and PM10) and its relationship with optical properties of aerosols over Delhi, India. *Atmos. Res.* 166, 223–232. doi:10.1016/j.atmosres.2015.07.007.

Van Donkelaar, A., Martin, R. V., Brauer, M., and Boys, B. L. (2015). Use of satellite observations for long-term exposure assessment of global concentrations of fine particulate matter. *Environ. Health Perspect.* 123, 135–143. doi:10.1289/ehp.1408646.

Vinoj, V., Rasch, P. J., Wang, H., Yoon, J., Ma, P., Landu, K., et al. (2014). Short-term modulation of Indian summer monsoon rainfall by West Asian dust. *Nat. Geosci.* 7. doi:10.1038/NGEO2107.

Vinoj, V., Satheesh, S. K., and Moorthy, K. K. (2010). Optical, radiative, and source characteristics of aerosols at Minicoy, a remote island in the southern Arabian Sea. *J. Geophys. Res. Atmos.* 115, 1–19. doi:10.1029/2009JD011810.

Wang, J., and Christopher, S. A. (2003). Intercomparison between satellite-derived aerosol optical thickness and PM2.5 mass: Implications for air quality studies. *Geophys. Res. Lett.* 30, 2–5. doi:10.1029/2003GL018174.

World Health Organization (2016). Ambient Air Pollution: A global assessment of exposure and burden of disease. *World Heal. Organ.*, 1–131. doi:9789241511353.

Xin, J., Gong, C., Liu, Z., Cong, Z., Gao, W., Song, T., et al. (2017). The observation-based relationships between PM2.5 and AOD over China Jinyuan. *J. Geophys. Res. Atmos.* 122, 3672–3685. doi:10.1002/2016JD025676.

Zhang, G., Rui, X., and Fan, Y. (2018). Critical review of methods to estimate PM 2.5 concentrations within specified research region. *ISPRS Int. J. Geo-Information* 7. doi:10.3390/ijgi7090368.

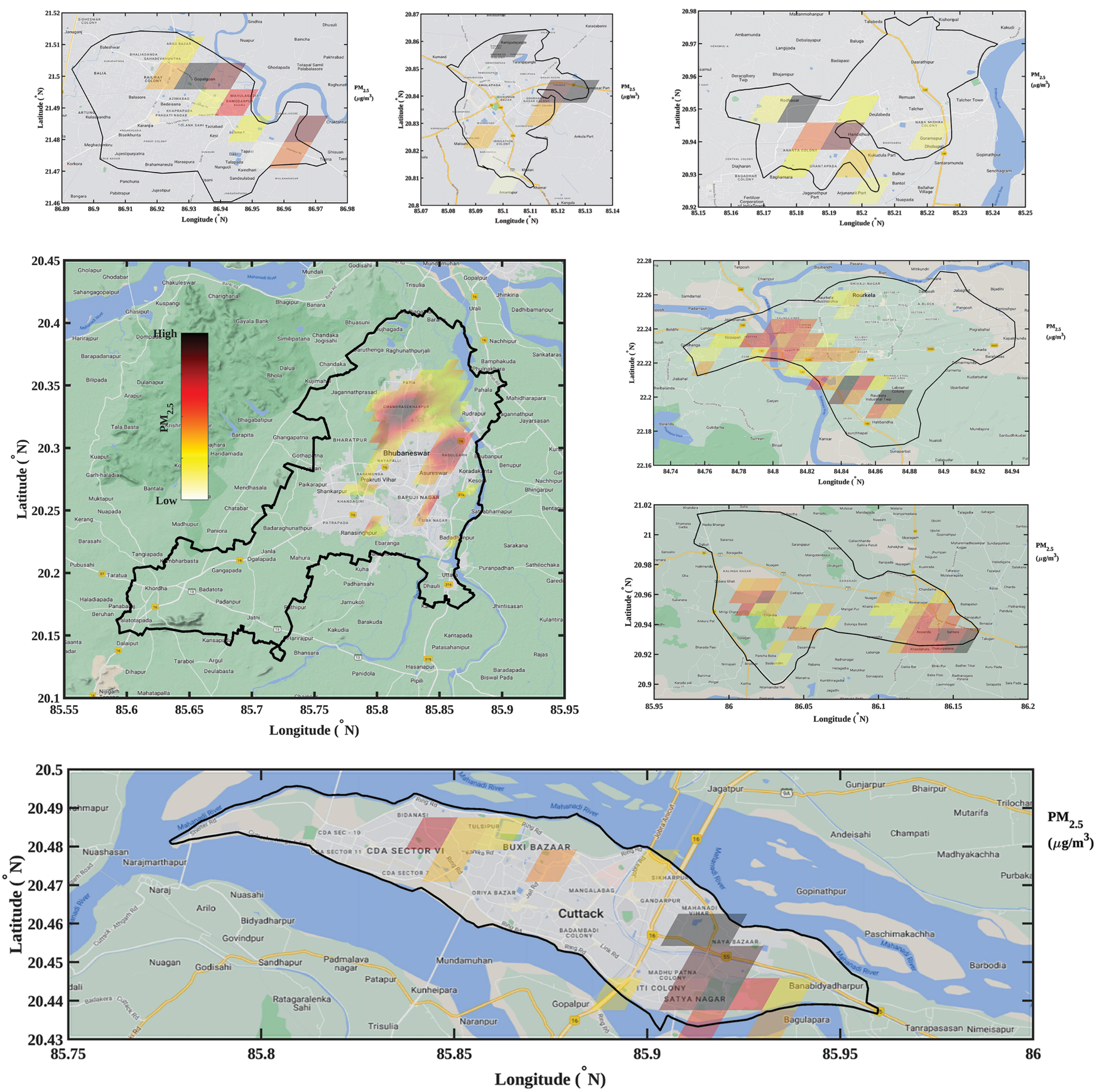

AEROSOLS, AIR QUALITY AND CLIMATE LAB

SCHOOL OF EARTH, OCEAN AND CLIMATE SCIENCES
INDIAN INSTITUTE OF TECHNOLOGY BHUBANESWAR

vinoj@iitbbs.ac.in